AD-A123 966 SHALLOW BULK ACOUSTIC WAVE (SBAW) DEVICES AND OSCILLATORS(U) TRW ELECTRONIC SYSTEMS GROUP REDONDO BEACH CA K V ROUSSEAU ET AL. NOV 82 DELET-TR-81-0415-1 1/1

UNCLASSIFIED DAAK20-81-C-0415 F/G 9/5 NL

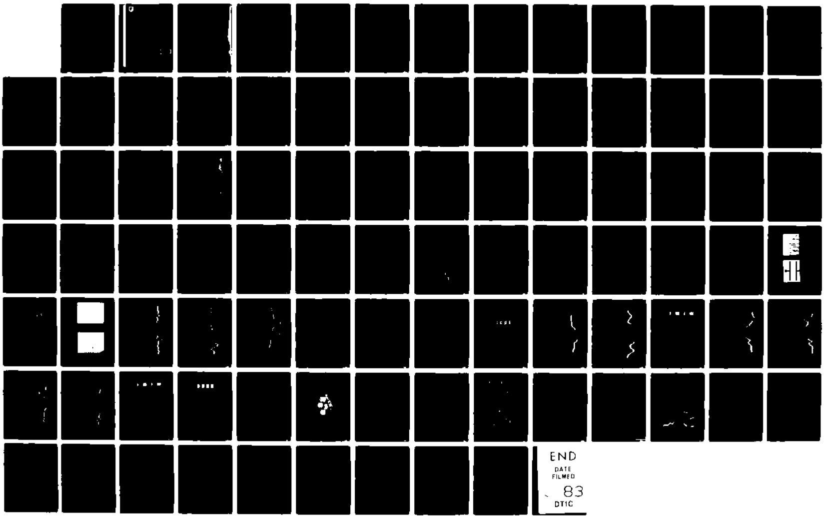

Research and Development Technical Report

DELET-TR-81-0415-1

AD A123966

SHALLOW BULK ACOUSTIC WAVE (SBAW) DEVICES AND OSCILLATORS

K. V. Rousseau, K. H. Yen, K. F. Lau and A. E. Faris
TRW Inc.
One Space Park
Redondo Beach, CA 90278

November 1982

Interim Report for Period 28 August 1981 - 28 August 1982

Approved for Public Release;
Distribution Unlimited

Prepared for:
ELECTRONICS TECHNOLOGY AND DEVICES LABORATORY

ERADCOM

US ARMY ELECTRONICS RESEARCH AND DEVELOPMENT COMMAND
FORT MONMOUTH, NEW JERSEY 07703

88 01 31 026

NOTICES

Disclaimers

The citation of trade names and names of manufacturers in this report is not to be construed as official Government endorsement or approval of commercial products or services referenced herein.

Disposition

Destroy this report when it is no longer needed. Do not return it to the originator.

REPORT DOCUMENTATION PAGE		READ INSTRUCTIONS BEFORE COMPLETING FORM
1. REPORT NUMBER: DELET-TR-81-0415-1	2. GOVT ACCESSION NO.: AD-A123 966	3. RECIPIENT'S CATALOG NUMBER
4. TITLE (and Subtitle): SHALLOW BULK ACOUSTIC WAVE DEVICES AND OSCILLATORS		5. TYPE OF REPORT & PERIOD COVERED: ~~Interim Report~~ 28 August 81 through 28 August 82
		6. PERFORMING ORG. REPORT NUMBER
7. AUTHOR(s): K. V. Rousseau, K. H. Yen, K. F. Lau and A. E. Faris		8. CONTRACT OR GRANT NUMBER(s): DAAK20-81-C-0415
9. PERFORMING ORGANIZATION NAME AND ADDRESS: TRW, Inc. Electronic Systems Group, One Space Park, Redondo Beach, CA 90278		10. PROGRAM ELEMENT, PROJECT, TASK AREA & WORK UNIT NUMBERS: 612705 H94.09.11.01
11. CONTROLLING OFFICE NAME AND ADDRESS: Director, US Army Electronics Tech & Dvcs Lab, ATTN: DELET-MA-A, Fort Monmouth, NJ 07703		12. REPORT DATE: November 1982
		13. NUMBER OF PAGES: 80
14. MONITORING AGENCY NAME & ADDRESS (if different from Controlling Office)		15. SECURITY CLASS. (of this report): Unclassified
		15a. DECLASSIFICATION/DOWNGRADING SCHEDULE

16. DISTRIBUTION STATEMENT (of this Report)

Approved for Public Release; Distribution Unlimited.

17. DISTRIBUTION STATEMENT (of the abstract entered in Block 20, if different from Report)

18. SUPPLEMENTARY NOTES

19. KEY WORDS (Continue on reverse side if necessary and identify by block number)

Shallow Bulk Acoustic Wave Devices
SBAW Oscillator
SH Surface Waves
Quartz

20. ABSTRACT (Continue on reverse side if necessary and identify by block number)

The objective of this program is to develop stable shallow bulk acoustic wave (SBAW) oscillators, stabilized directly at L through X band frequencies. This first annual report describes the technical progress of the program for the period of September 1981 to August 1982. The major activities for this period were the examination of system applications of SBAW oscillators, SBAW device investigation, device fabrication, and oscillator circuit design. The parameters studied in the SBAW device investigation were material aspects,

(continued)

metallization effect, transducer configuration, equivalent circuit, and harmonic operation. Device fabrication has concentrated on delay lines operating at frequencies from 3 to 5 GHz, and results have been obtained for device mounting and packaging. SBAW oscillator circuit designs have been developed and are in fabrication.

Several systems have been identified in which the use of high frequency SBAW devices will greatly improve system performance. From the system study, it is clear that as more and more weapon systems move to millimeter wave, there will be an increasing requirement for stable, low noise frequency sources and precision test equipment. SBAW technology will provide the devices which will be needed to meet this challenge.

TABLE OF CONTENTS

LIST OF FIGURES

LIST OF FIGURES (Cont'd)

LIST OF FIGURES (Cont'd)

LIST OF TABLES

1.0 INTRODUCTION

The objective of this program is to develop low phase noise Shallow Bulk Acoustic Wave (SBAW) oscillators, stabilized directly at L through X bands, with emphasis on higher frequency of operation, improved temperature stability and good long-term aging behavior. This first annual report describes the technical progress of this program for the period of September 1981 through August 1982. The major activities for this period were the SBAW device investigation, SBAW device fabrication, and examination of system applications and considerations for SBAW oscillators. System implementation of SBAW oscillators is examined in Section 2. Section 3 discusses results of the device investigation, where emphasis was placed on parameters governing SBAW device performance at frequencies above 2 GHz. These parameters include material aspects, metallization effect, transducer configuration, equivalent circuit, and harmonic operation. Section 4 describes the device fabrication, mounting and packaging. Section 5 describes preliminary SBAW oscillator circuit design, and Section 6 presents conclusions and future plans.

2.0 SYSTEMS STUDY

Recent years have seen the development of weapon systems with sophisticated tracking and targeting capabilities. To obtain high resolution, most of these systems employ infrared or laser sensors. With the increasing capabilities at millimeter wave, many systems are being designed or redesigned using millimeter wave sensors. These sensors provide better performance in adverse weather and bad visual conditions than the current sensors.

A key requirement for many millimeter wave systems is a stable frequency source. In the interests of minimizing the inevitable 20 log n phase noise degradation caused by frequency multiplication, it is highly desirable that the stable frequency source operate at as high a frequency as possible. Coherency is also an important requirement for many of these systems. This makes it necessary for the frequency source to meet the systems stabili v requirements.

SBAW oscillators meet all of these requirements. They are le frequency sources since they are based on a crystal technology. W oscillators are being fabricated at frequencies up to 10 GHz, yi ; a 40 dB improvement in phase noise over a multiplied 100 MHz fundamental mode crystal oscillator. SAW and SBAW voltage controlled oscillators can be built to lock to system requirements with current implementation methods.

2.1 IMPLEMENTATION

Performance requirements for SBAW oscillators depend on their implmentation into systems. For the systems discussed, these can be broken into coherent, noncoherent, MEDFLI, and ANA implementations.

A conventional frequency source under consideration for coherent systems such as HAWTADS, WASP, SRHIT and STARTLE is seen in Figure 2-1. The stable source is a 100 MHz crystal oscillator. Phase noise is considerably increased by the multiplication factor required.

Contrasted with this is the SBAW-based frequency source shown in Figure 2-2. A 7.8 GHz SBAW phase-locked oscillator has replaced the transistor phase-locked oscillator. This maintains coherence, while improving the phase noise performance. This is illustrated in Figure 2-3, which shows the relative phase noise performance of the conventional and the SBAW-based. Use of this SBAW-based source would improve the system performance of coherent millimeter wave weapon systems.

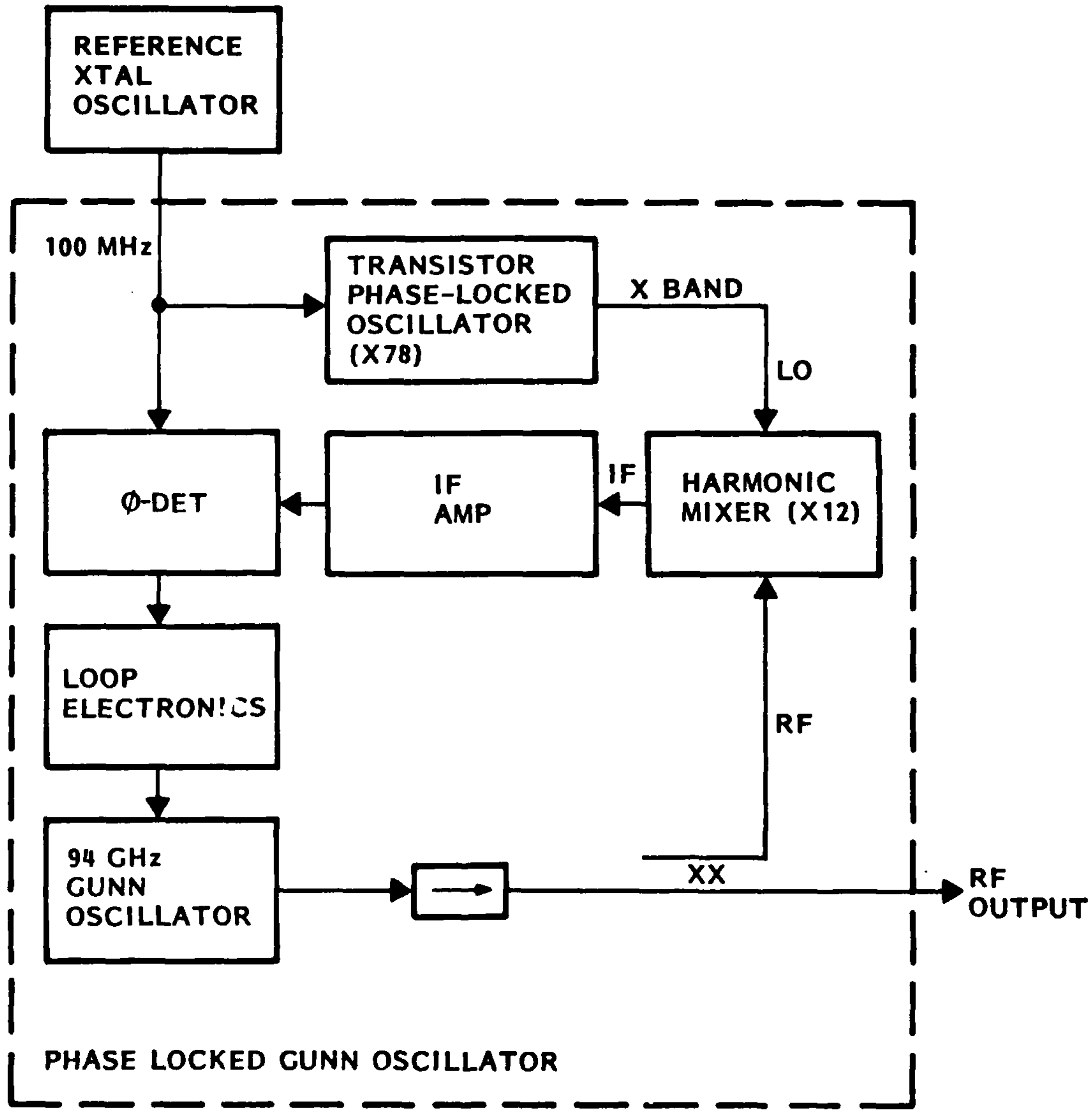

Figure 2-1. Simplified Block Diagram of Conventional CW Gunn Phase-Locked Oscillator

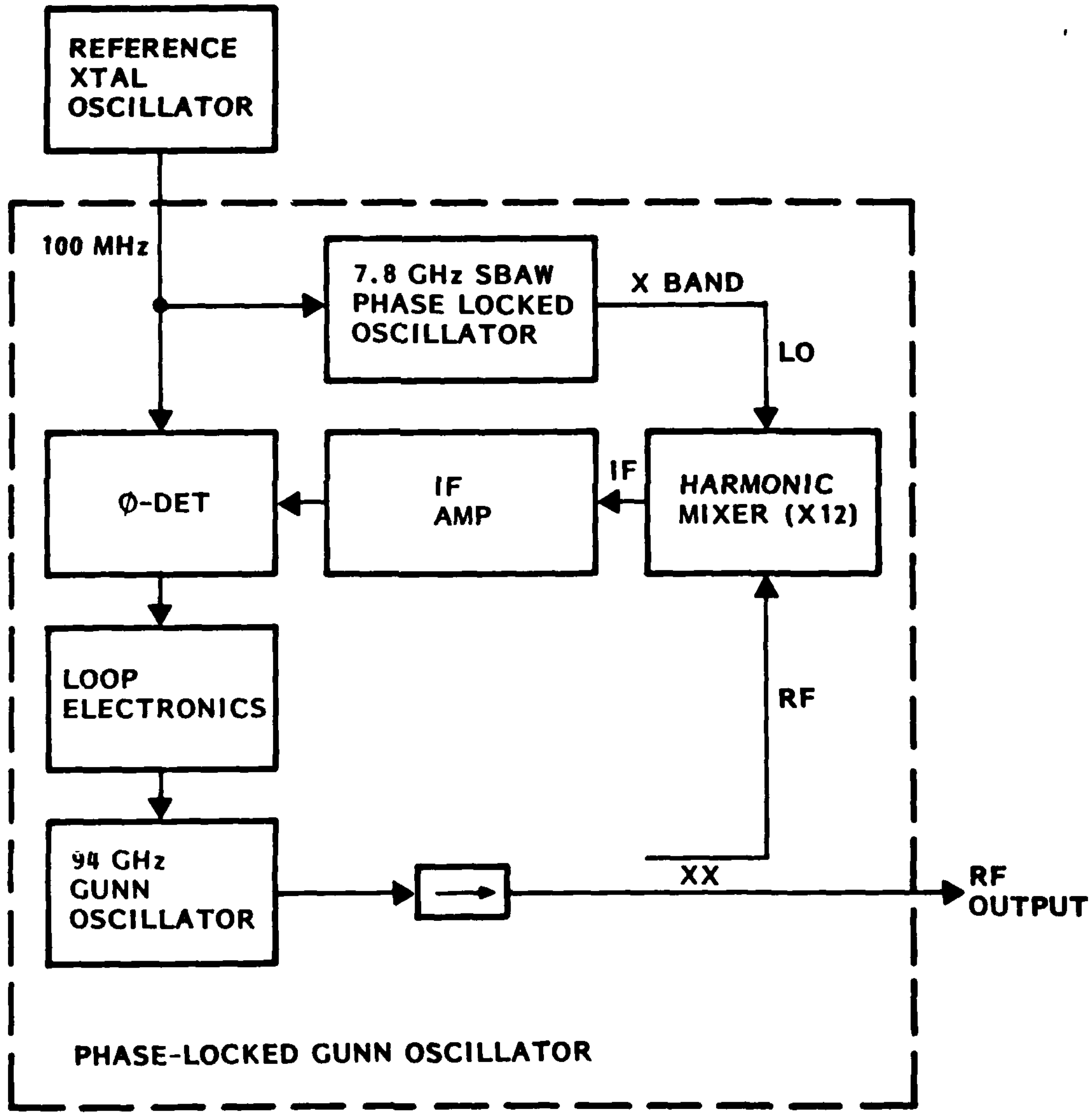

Figure 2-2. Simplified Block Diagram of SBAW-Based Gunn Phase-Locked Oscillator

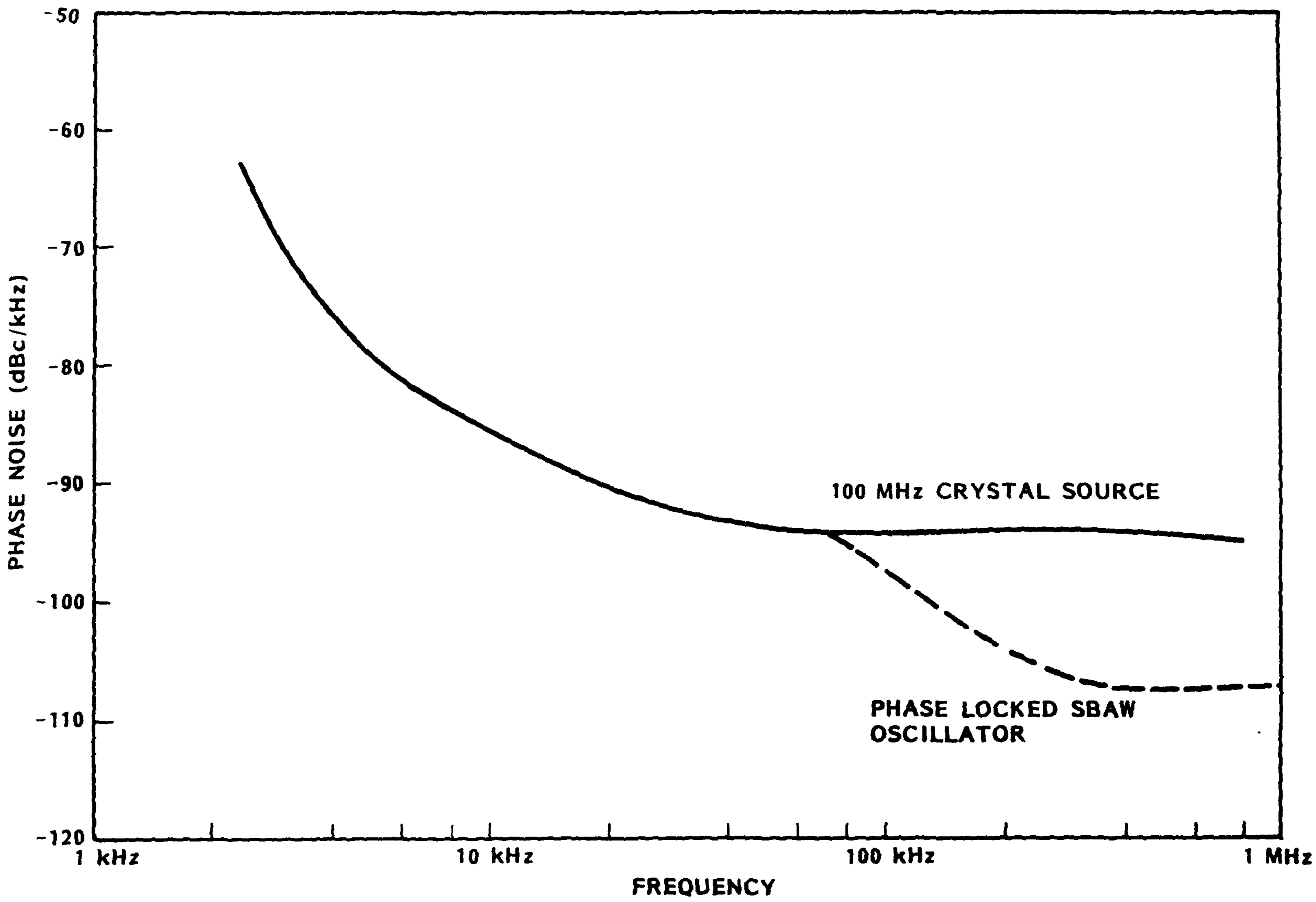

Figure 2-3. Phase Noise Response, 100 MHz Crystal vs. SBAW Oscillator

Another comparison that may be of interest is examining the phase noise of a state-of-the-art 10 MHz commercially available quartz bulk oscillator, shown in Figure 2-4. The 10 MHz oscillator is referred to 3.5 GHz, resulting in the familiar 20 log n increase in phase noise of a multiplied source. It has a noise floor of roughly -110 dBc. The 3.5 GHz SBAW oscillator has significantly poorer close-in phase noise, but a noise floor of -141 dBc, based on the assumptions of 30 dB loop gain (implying a device with insertion loss in the range 26-27 dB) and an amplifier with a 3 dB noise figure. *The* $1/f_m^2$ *dependence ends at a frequency* $f_\tau = 1/2\pi\tau$, where τ is the group delay.[1] Here, a Q of 1000 was assumed, giving $f_\tau \approx 1.75$ MHz. The "flicker" noise region, shown by the dashed line, has a $1/f_m^3$ dependence, and occurs in the close-in region. It must be determined experimentally, and the line on the graph represents an educated guess based on phase noise measurements of a 3.4 GHz SBAW oscillator developed at TRW.[2] Clearly, for high-frequency microwave sources, SBAW oscillators, perhaps injection-locked by a bulk oscillator, represent a significant improvement where phase noise is concerned.

Frequency sources for noncoherent systems are easier to implement than those for coherent systems. In fact, free running oscillators are used, or expected to be used, in many noncoherent systems such as SADARM. This provides acceptable performance, but SAW or SBAW oscillators provide the performance improvement of frequency stable, low noise sources at a small additional cost in quantity production.

The MEDFLI system provides many opportunities for SAW/SBAW implementations. In the front end, a stable LO is required for millimeter wave down conversion. Frequency synthesizers, both at 3-17 GHz and fast-hopped at 2.5 to 3 GHz also can be based on SAW/SBAW technology. Finally, the 2.01 GHz LO could use SAW/SBAW technology.

Figure 2-5 shows the proposed millimeter adapter for the automatic network analyzer. The two phase-locked sources would be implemented as SBAW phase-locked oscillators at 7 GHz, followed by X5 multipliers. Since this is a measurement system, high stability and low phase noise are required.

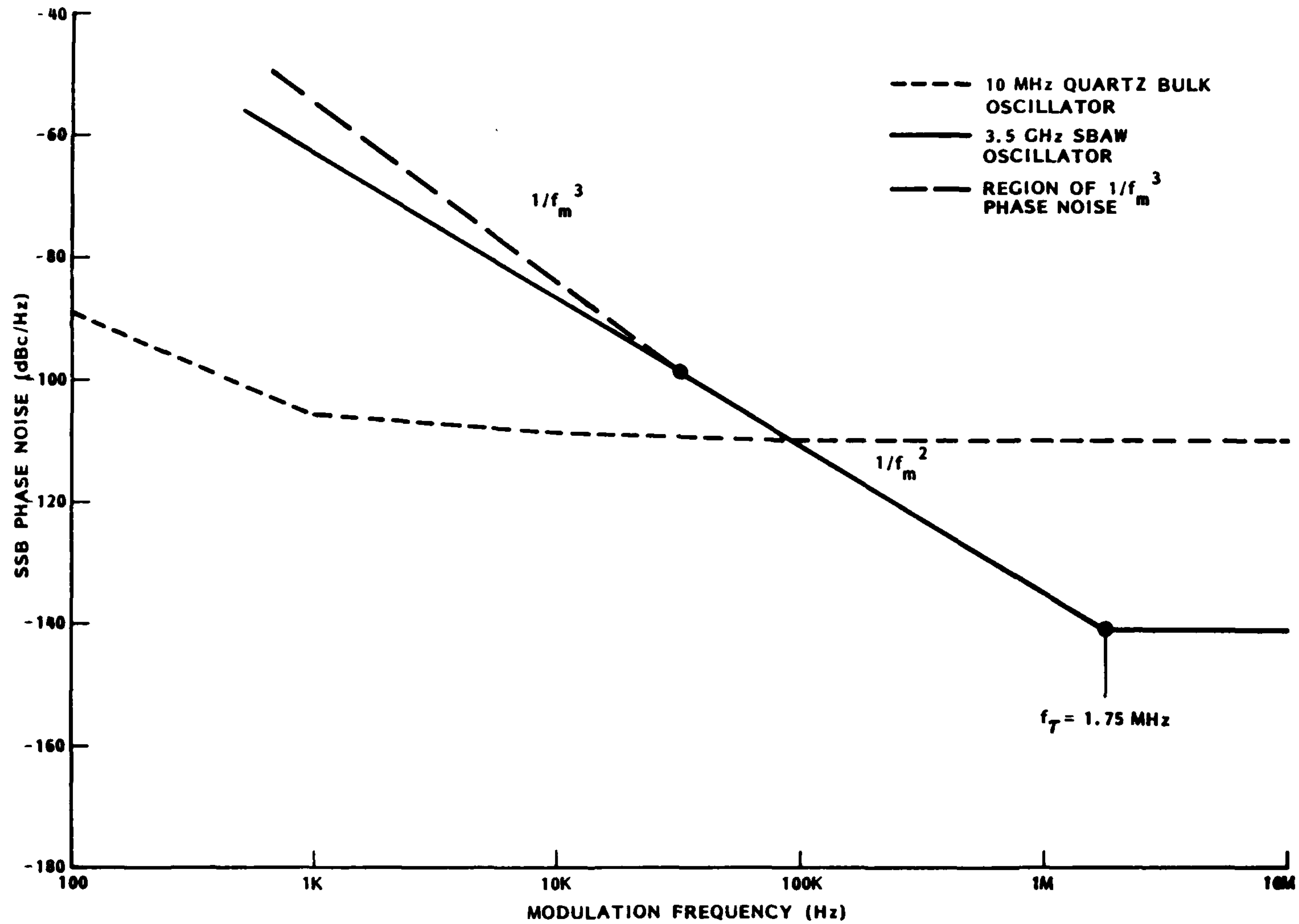

Figure 2-4. Comparison of Multiplied Bulk Resonator vs. Direct SBAW Phase Noise

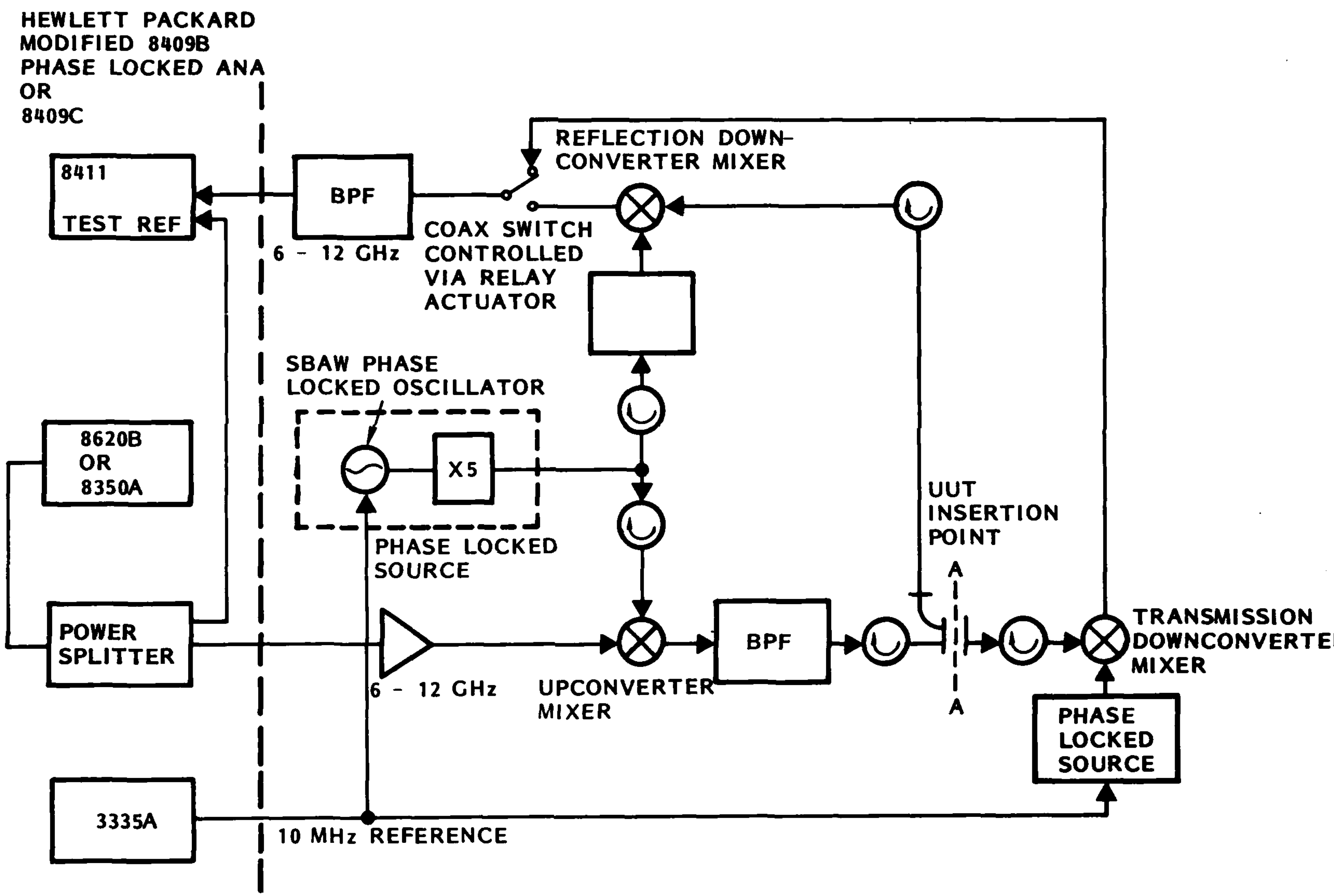

Figure 2-5. Proposed Millimeter Wave (41-47 GHz) Adapter

3.0 SBAW DEVICE INVESTIGATION

The activity in this area investigates key parameters governing SBAW device performance at high frequencies. These parameters include material aspects, metallization effect, transducer configuration, equivalent circuit and harmonic operation. The result of this investigation provides design techniques of optimum SBAW devices for stable high frequency oscillators.

3.1 MATERIAL ASPECTS

3.1.1 SBAW Materials

Shallow bulk acoustic waves are essentially bulk waves which propagate along the crystal surface.[3] They can be launched and detected with interdigital transducers (IDTs). In rotated Y-cut quartz, the wave is a pure shear plane wave with polarization parallel to the surface and perpendicular to the direction of propagation. While the group velocity vector must be parallel to the surface for most efficient transmission, the phase velocity vector generally points in another direction.

On doubly rotated cuts of quartz, the acoustic field is more complicated since the longitudinal and two shear bulk modes are usually excited simultaneously. SBAWs have been found on doubly rotated cut quartz; an example is the $\phi = 10°$, $\theta = +34°$ cut with propagation in the Z direction, which presents three modes having velocities of 1873, 2521, and 3177 m/s.[4-6] Doubly rotated cuts may provide improved temperature stability and thermal stress compensation for SBAWs as they do for bulk waves in the SC-cut. While SBAW propagation has been observed in doubly rotated cut quartz, a full understanding of its properties has yet to be established.

Berlinite has the same symmetry as quartz and can be analyzed similarly. Other substrates, such as $LiNbO_3$ and $LiTaO_3$, require different orientations for SBAW propagation.[3] Also, they do not have good temperature stability for frequency source applications.

Of the four materials discussed, only quartz and berlinite have the required temperature stability. The wave velocity of SBAW on quartz is approximately 1.2 times higher than that of berlinite, and the crystal quality of berlinite is presently not suitable for device applications. Quartz is therefore the logical choice. The SBAW in quartz has been extensively investigated, and it has been shown that for good temperature stability the available quartz SBAW substrates are near 35.5° and -50.5° rotated Y-cut quartz. Table 3-1 compares the properties of these two substrates.

3.1.2 SBAW Viscous Attenuation

The viscous loss for bulk waves in rotated Y-cut quartz has been given by Slobodnik.[7] This loss was calculated theoretically from the wave strains through the viscosity tensor. The predicted attenuation for AT-cut quartz is less than one-third (in dB) of that for SAWs on ST-X quartz. Viscous loss (in dB) is proportional to frequency squared. For a SBAW delay line on AT or BT-cut quartz with a total path length of 500 wavelengths, the viscous attenuation at various frequencies is shown in Table 3-2.

Table 3-2. SBAW Viscous Attenuation in AT- and BT-Cut Quartz

	AT-Cut Quartz		BT-Cut Quartz	
Frequency	SBAW Attenuation	Loss at 500 Wavelengths	SBAW Attenuation	Loss at 500 Wavelengths
1 GHz	0.87 dB/μs	0.44 dB	2.0 dB/μs	1.0 dB
2 GHz	3.5 dB/μs	0.85 dB	8.0 dB/μs	2.0 dB
5 GHz	22 dB/μs	2.2 dB	50.0 dB/μs	5.0 dB
10 GHz	87 dB/μs	4.4 dB	200.0 dB/μs	10.0 dB

This calculation shows that, in terms of material parameters: SBAW devices are feasible at very high frequencies.

Table 3-1. Comparison of SBAW Properties Between +35.5° and -50.5° Rotated Y-Cut Quartz

	Substrate Angle	
	+35.5°	-50.5°
Wave Velocity	5100 m/sec	3331 m/sec
Coupling Coefficient	1.44×10^{-2}	0.4×10^{-2}
Mass Loading Effect for $H/\lambda = 0.01$	$\Delta v/v = 0.16\%$	$\Delta v/v = 0.01\%$
Wave Attenuation at 1 GHz	0.87 dB/μsec	2.0 dB/μsec
Uniform Isotropic Static Stress ($\times 10^{-12}$ M^2/N)	2	-7
Temperature Stability (-55°C to -85°C)	± 127 ppm	± 55 ppm

3.1.3 Static Stress on SBAW

Crystal relaxation is a very important aging mechanism for SBAW devices as well as SAW devices. The rate for this aging mechanism, will, of course, depend on the crystal cut. For material selection, the stress effect on SBAW device aging has been calculated assuming an isotropic film stress on rotated Y-cut quartz. The result is shown in Figure 3-1. A stress of 1×10^{16} N/m^2 will produce a frequency variation of about 2 ppm on AT-cut quartz. As shown in Figure 3-1, SBAWs on AT quartz are only one-sixth as sensitive to isotropic film stress as SAWs on ST-cut quartz and one-twelfth as sensitive as shear waves in AT or BT bulk quartz resonators.

From the above discussions, it is clear that near +35.5° cut quartz has the advantage of high wave velocity, high coupling coefficient, low wave attenuation and low static stress effect. The only disadvantage is its sensitivity to the metal loading effect, which will be discussed in Section 3.2. However, this sensitivity to metal loading can also be an advantage since it provides a means for frequency trimming. The -50.5°, on the other hand, has the advantage of better temperature stability and potentially better device aging characteristics because it has a smaller mass loading effect. The overall properties of the 35.5° cut make it a more attractive substrate for high frequency device application unless the applications require high temperature stability. For this program, the primary candidate, therefore, will be a substrate with a rotation angle near +35°.

3.2 METALLIZATION EFFECT ON SBAW PROPAGATION

The theory of SBAW propagation on the free surface of quartz has been analyzed at TRW.[3] The analysis ignored electrical and mechanical loading effects of interdigital transducers. Good agreement between theory and experiment has been obtained for low frequency SBAW delay lines operating at frequencies up to several hundred megahertz. However, metal films, either on top of the surface or embedded in grooves, are necessary for interdigital transducers. In high frequency operation, the effects of these metal films cannot be ignored. They are known to convert a SBAW into a shear horizontal surface wave and to slow the wave, pulling it more closely to the surface and improving coupling. In addition, they alter

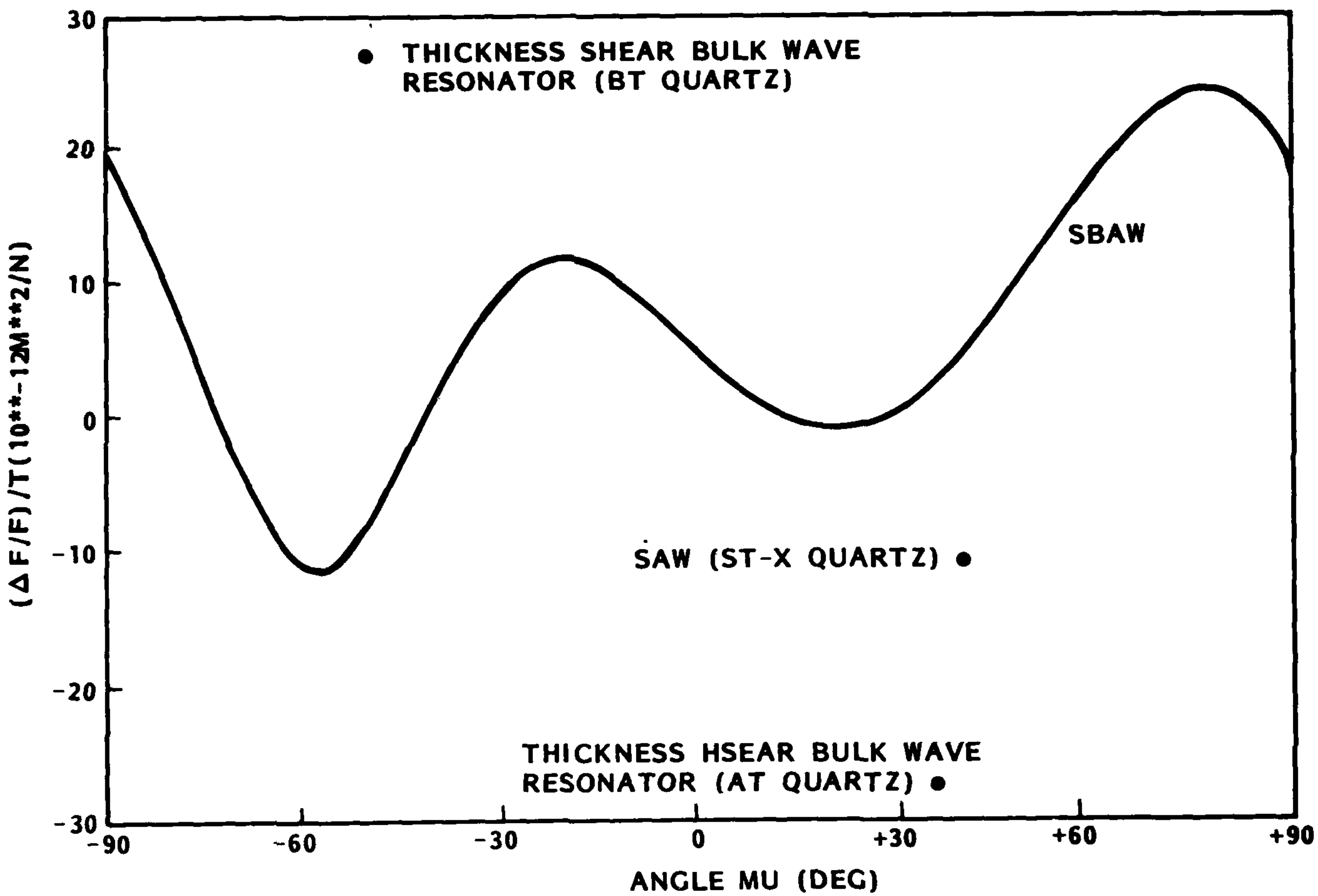

Figure 3-1. The Effect of Uniform Isotropic Static Stress in the Plane of the Surface for SBAW, SAW and Bulk Wave Resonators on Quartz.

the device temperature characteristics and cause diffraction at the ends of the transducers. A detailed understanding of the metallization effect is therefore essential for the design of SBAW delay lines.

Since an IDT produces a periodic electrical and mechanical loading effect on the substrate surface, it is extremely difficult to obtain an exact solution regarding its loading effects. Therefore, an approximate IDT model, assuming a layered surface of effective thickness H_0 as shown in Figure 3-2 was used for the analysis.[8] This approach is valid only if the propagation path between transducers is very short, as in the case of single mode delay line oscillators, or layered with a metal film as an energy trapping structure. This subsection therefore describes calculated and experimental results for metallization effects on SBAW devices.

3.2.1 Phase Velocity

The method of theoretical analysis of shear horizontal surface waves is given in Reference (9). The calculated phase velocity on rotated Y-cut quartz is shown in Fig. 3-3 for an aluminum layer with $H/\lambda = 0.01$ (where H is the aluminum thickness and λ is the wavelength), and Figure 3-4 shows the velocity change $\Delta V/V_m$ for $H/\lambda = 0.01$, where $\Delta V = V_{SBAW} - V_m$. The velocity change near AT-cut quartz is larger than that near BT-cut quartz. For quartz, a metal film at high frequencies is a much stronger perturbing force than the electrical boundary conditions alone. The SH surface waves produced under the metal film of an IDT at high frequencies are therefore stronger, significantly slower, and more closely bound to the surface than the B-G waves generated by line charge excitation on a free surface.

The slowing of the SH surface wave by a metal film affects the overall device frequency. Figure 3-5 shows theoretical and experimental results relating device frequency to metal thickness in a nominally 2 GHz delay line oscillator with recessed fingers. The theory was calculated with an approximate IDT model. The difference in theory and experiments is attributed to uncertainty in transducer film thickness, groove depth and finger aspect ratio. At high frequencies, film thickness control is therefore critical in achieving the desired frequency of operation.

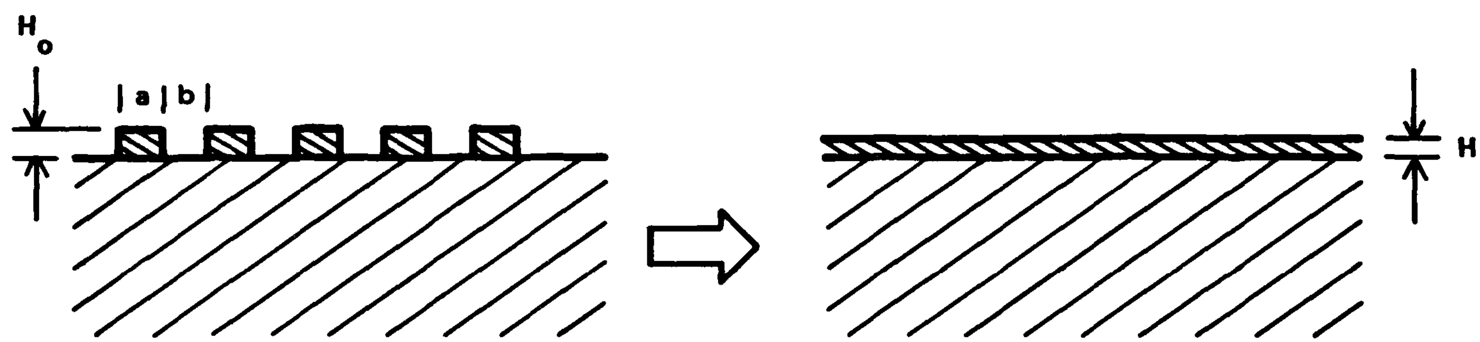

$$H = \frac{a}{a + b} H_o$$

Figure 3-2. First Order Approximation of IDT Model
Aspect Ratio = $\frac{a}{a + b}$.

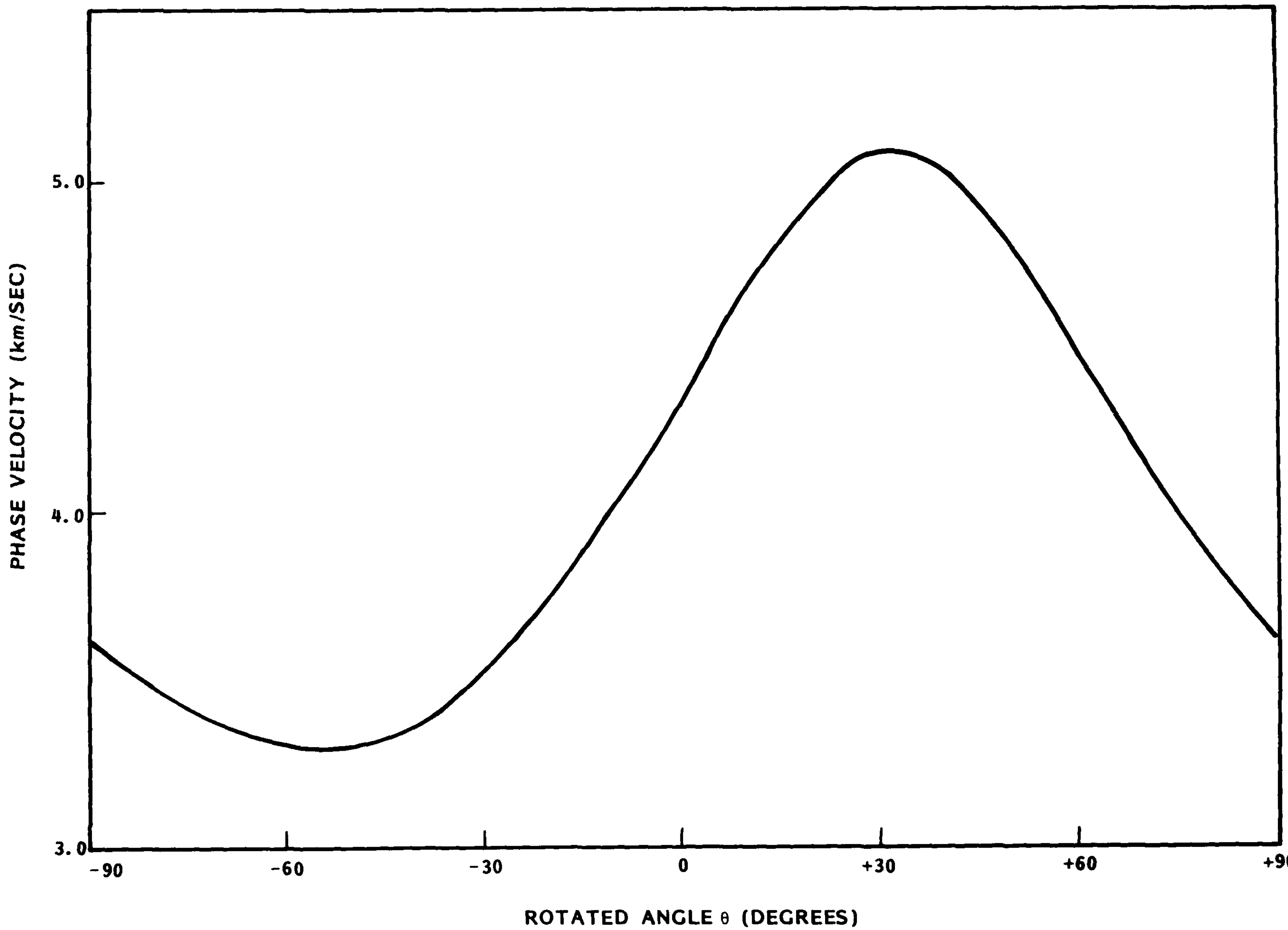

Figure ?-3. Phase Velocity as a Function of Rotated Angle for Aluminum Thickness H = 0.01λ

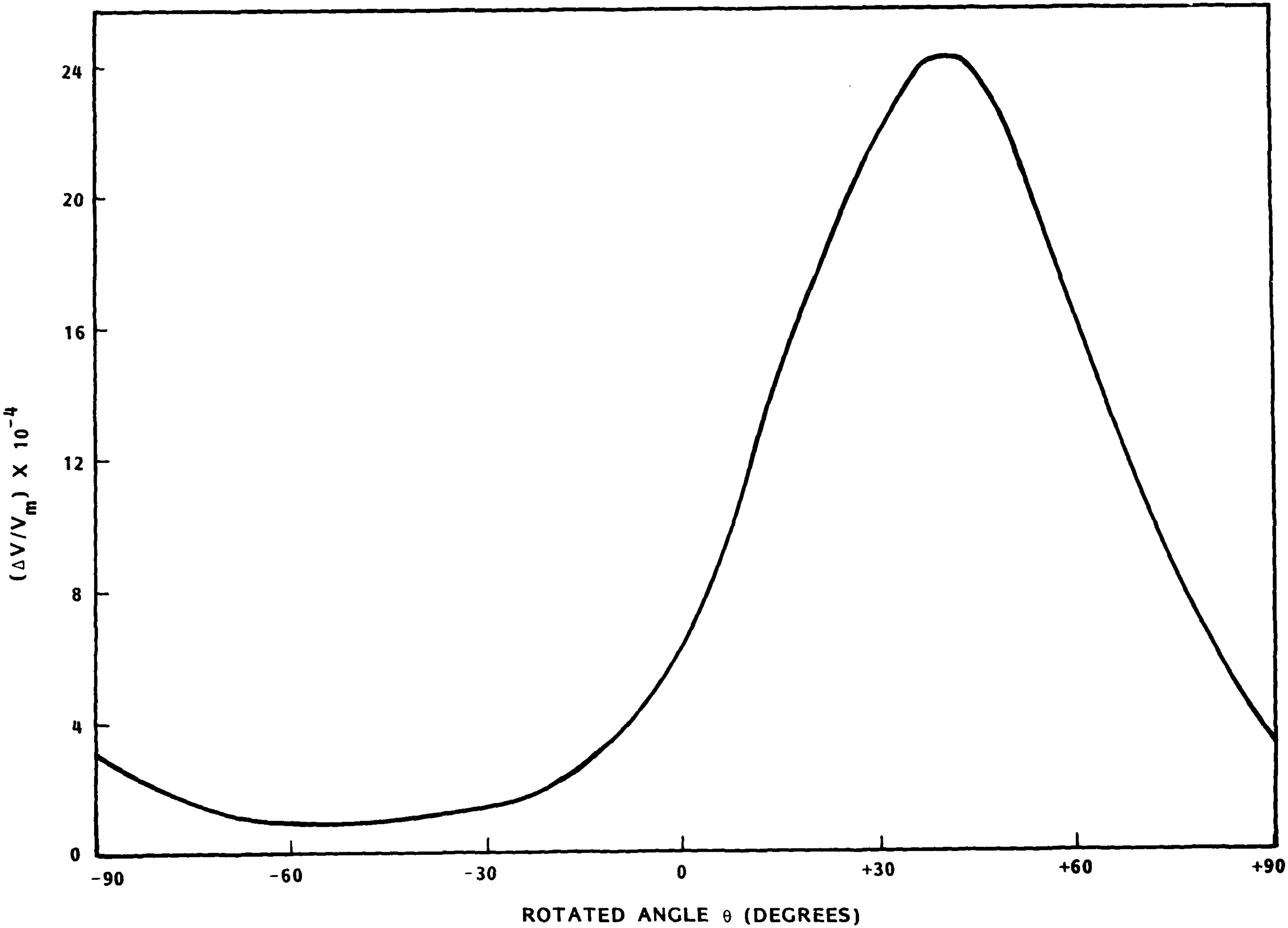

Figure 3-4. Velocity Change as a Function of Rotated Angles (Aluminum H/λ=0.01)

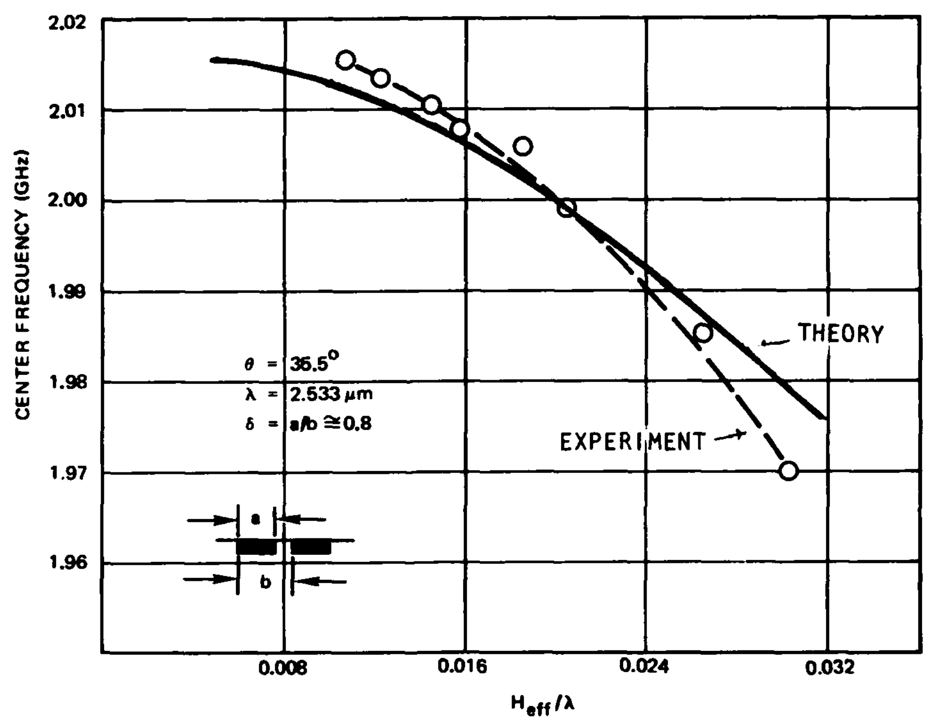

Figure 3-5. Dependence of Center Frequency Upon Normalized Metal Film Thickness

It is known that one important aging mechanism for SBAW devices is stress relaxation of the electrodes. Metal film stress can be minimized by the use of gold film, which has low intrinsic stress. Thus, the mass loading effect of gold film was calculated in an attempt to employ gold film transducers for low aging delay lines.

Figure 3-6 shows the calculated phase velocity of SH surface waves as a function of rotated angle on quartz with gold film thickness of $H = 0.01\lambda$. It is seen that the mechanical loading effects of a gold layer are very large compared with those of Al, because the shear wave velocity of gold ($\sim$ 1250 m/sec) is very low, and the density of gold is very large. The velocity change $\Delta V = V_{SBAW} - V_m$ is about 13% near 36° rotated Y-cut quartz. This large mechanical loading effect makes gold film not suitable for high frequency SBAW devices. For example, Figure 3-7 shows the frequency response of a 1 GHz SBAW delay line using gold film transducers. The result shows that the insertion loss is about 10 dB higher and the center frequency is about 20 MHz lower than those of identical delay lines using aluminum film transducers.

3.2.2 Temperature Stability

As in SAW devices, a metal film also alters the turnover temperature of SBAW devices. This effect is due to the temperature dependence of the film's elastic properties. Figure 3-8 shows the calculated temperature-frequency behavior of a SBAW device on 36.75° rotated Y-cut quartz with thin aluminum films. It is seen that the turnover temperature shifts from T = 55°C at $H/\lambda = 0.012$ to T = 22°C at $H/\lambda = 0.024$ (solid lines). Also shown in Fig. 3-8 are the previously measured and calculated results (denoted by dots and dashed line). The temperature-frequency behavior was measured using a 2 GHz SBAW oscillator, while the calculated result (dashed line) was for a free surface alone. Good agreement between theory and experiment was obtained when metallization effect was included in the model (dots and solid line). The turnover temperature is seen to be lowered by as much as 30°C for a 2 GHz oscillator.

The turnover temperature of a SBAW delay line depends not only on transducer metallization thickness, but also on the aspect ratio of finger width and gap spacing. This is because the effective film thickness is a function of transducer aspect ratio, as illustrated by the approximate IDT model shown in Fig. 3-2. The turnover temperature as a function of aluminum film thickness H/λ is shown in Fig. 3-9 for devices on 36.75° rotated

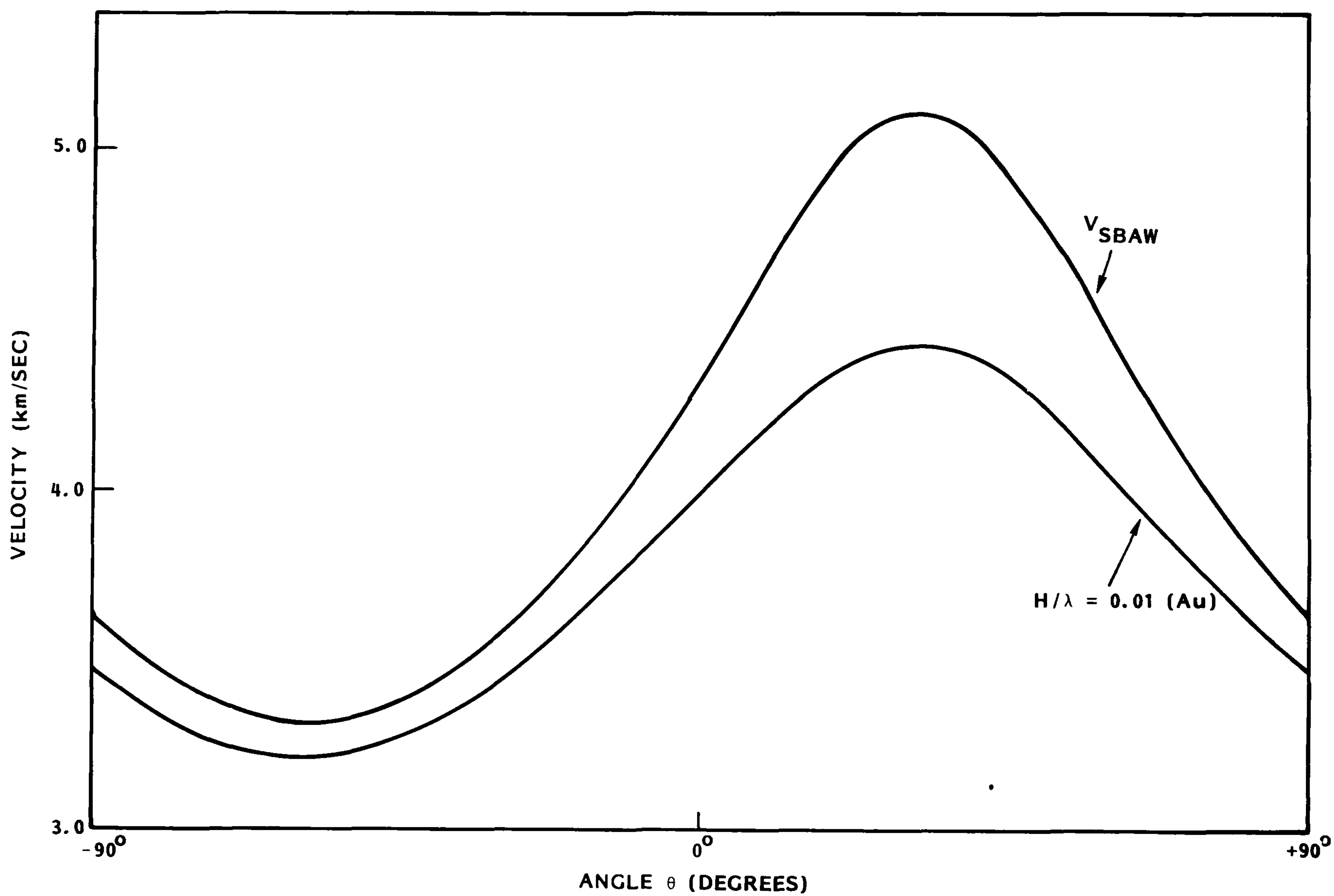

Figure 3-6. SH-Wave Velocity as a Function of Rotated Angle on Quartz with Gold Metallization

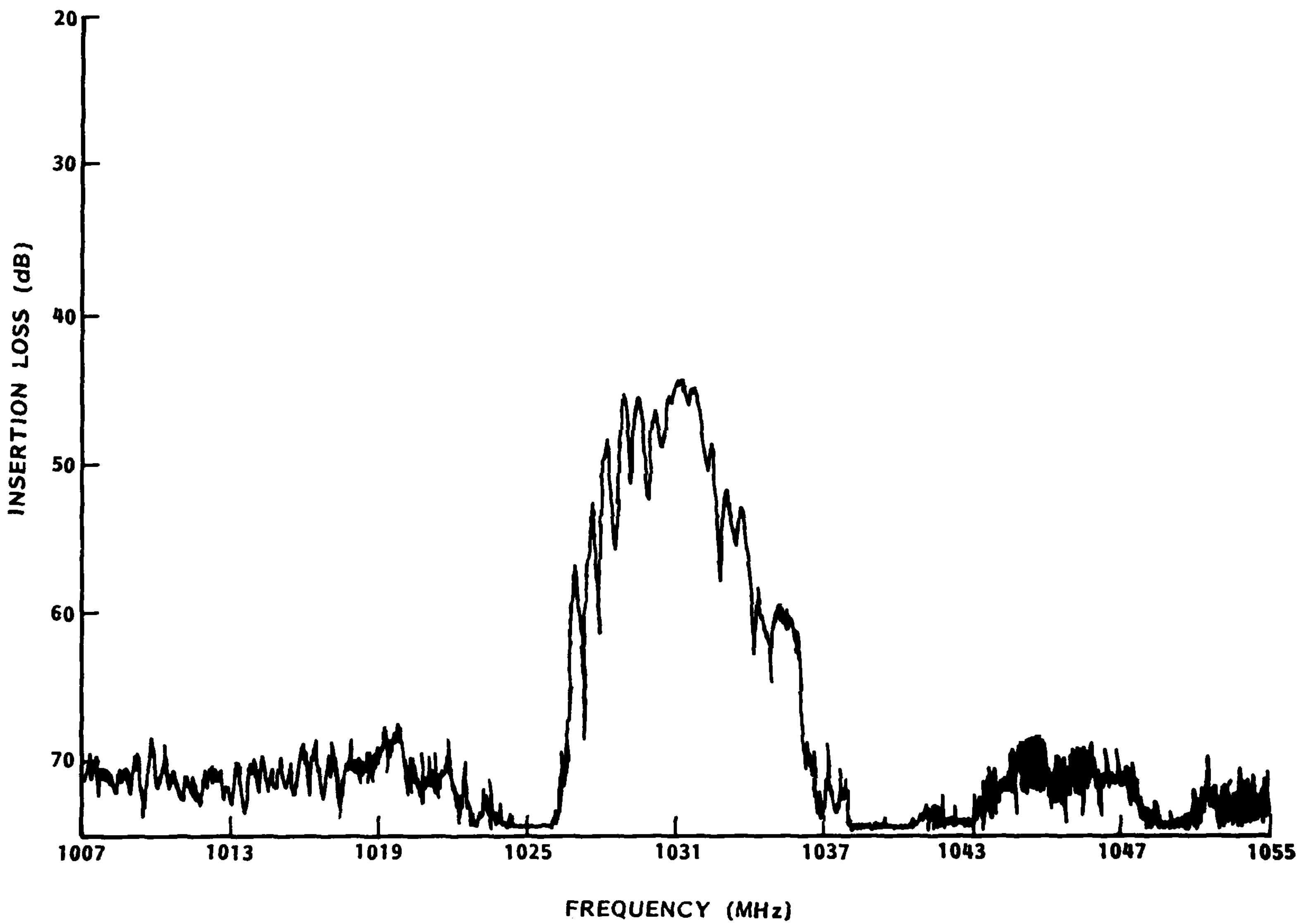

Figure 3-7. Frequency Response of a SBAW Delay Line with 300-400 Å Gold Transducers (Unmatched)

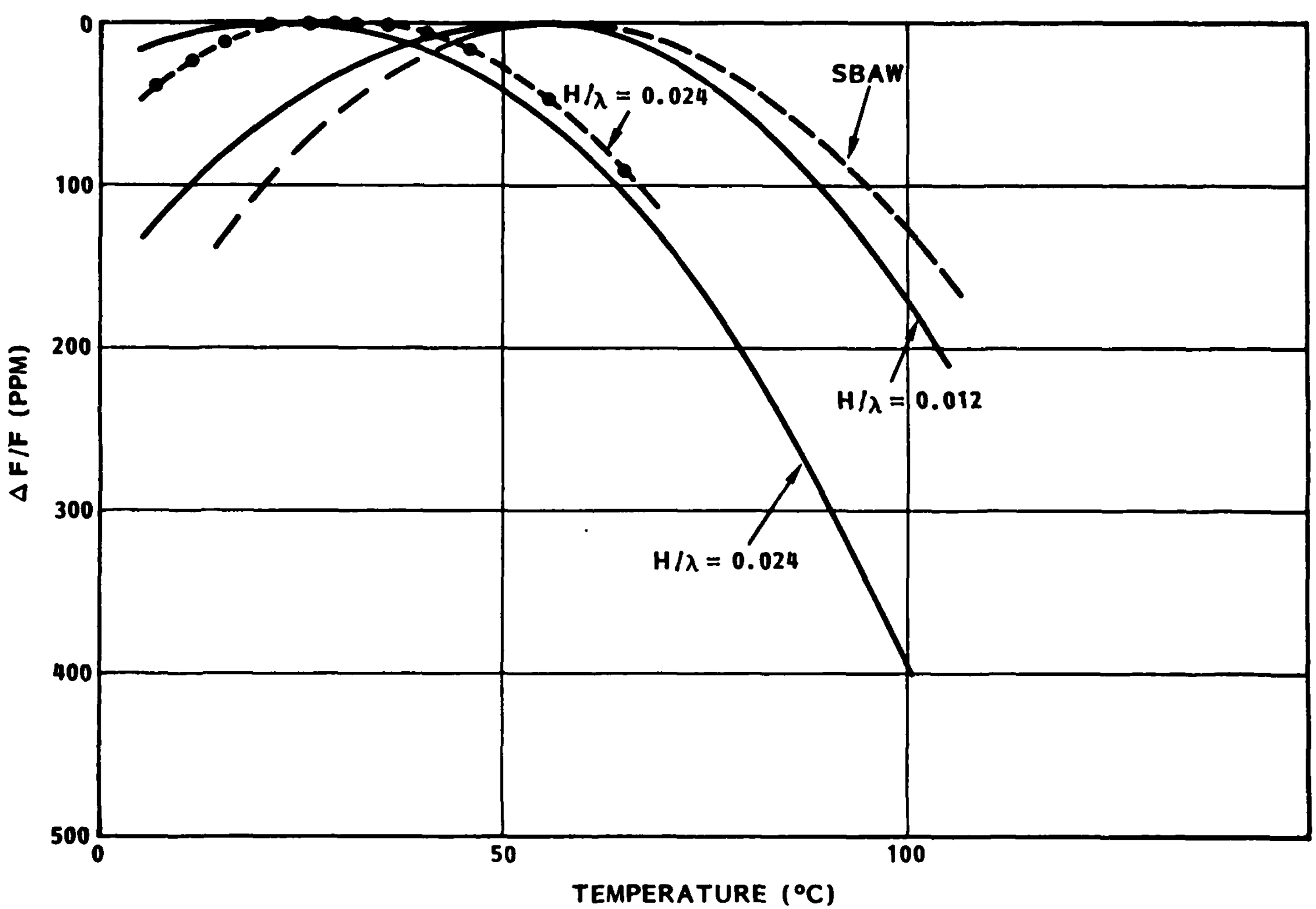

Figure 3-8. Temperature Behavior of SBAW Delay Line on 36.75° Rotated Y-Cut Quartz

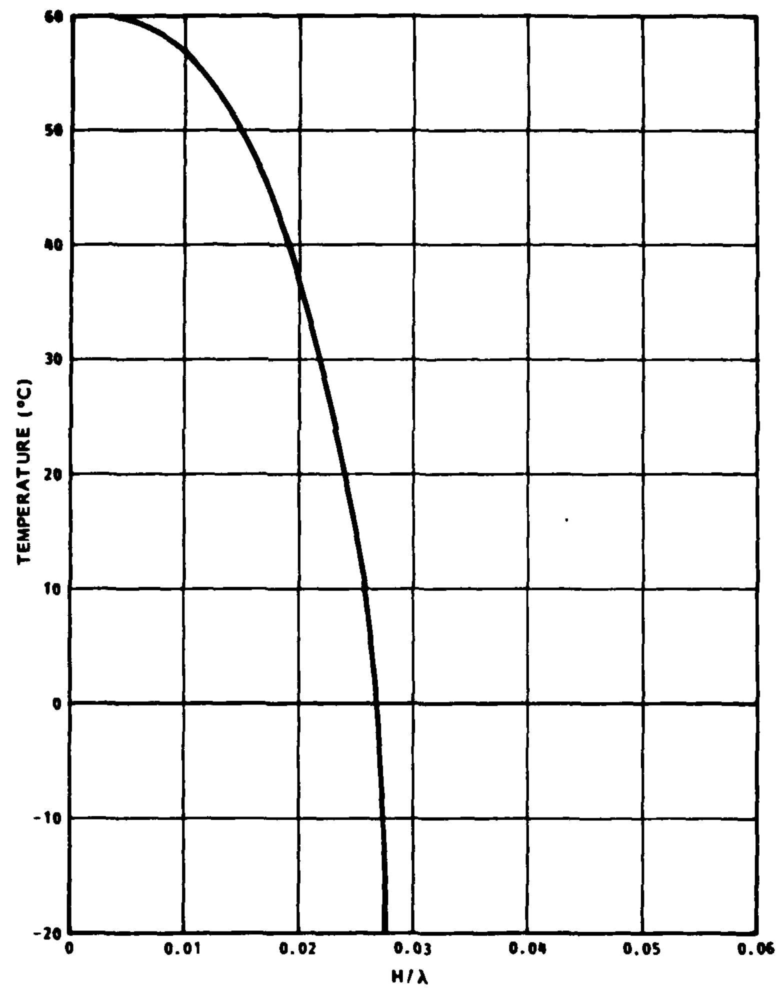

Figure 3-9. Turnover Temperature as a Function of Normalized Film Thickness (θ = 36.75°)

Y-cut quartz. It is seen that the turnover temperature varies over 100°C as H/λ varies from 0.01 to 0.03. Thus, control of the aluminum film thickness as well as the aspect ratio of transducers is critical in achieving the desired frequency-temperature behavior.

Figure 3-10 shows the turnover temperature as a function of rotated angle for $H/\lambda = 0.015$. This H/λ value corresponds to a transducer having aluminum thickness of 500 Å and aspect ratio of 0.5 for a 3 GHz delay line ($\lambda = 1.6$ μm). Note that 36.25° rotated Y-cut quartz has a turnover temperature near room temperature and will be used for 3 GHz SBAW delay lines.

For completeness, the effect of gold film on turnover temperature was also calculated as a function of rotated angles in Fig. 3-11 for $H/\lambda = 0.01$ and 0.015. It is seen that the change in turnover temperature is quite large for only a small change in gold film thickness. This effect also rules out the use of gold film for high frequency devices.

3.2.3 Propagation Loss

The propagation loss due to viscous attenuation increases when metal films are involved. Metals have considerably higher propagation loss than quartz. The effect of this high material loss on overall propagation loss will depend on the fraction of acoustic power flow that passes through the film. Since the choice of optimum delay time for the SBAW delay line depends critically on the propagation loss, the propagation loss must be evaluated in structures which simulate the actual structure of a SBAW transducer.

The SBAW is a horizontal shear wave whose particle motion is in the plane of the substrate. Laser probing of the surface for evaluating propagation loss is not useful because no diffraction of the laser beam can be detected. As a result, conventional techniques based on transducers were used to evaluate propagation loss of SBAW. For experiments, a pair of SBAW delay lines with the same transducer design, but different transducer separation, was fabricated simultaneously, as shown schematically in Fig. 3-12. The gaps between the transducers are filled with structures simulating the SBAW transducer. Since both devices are fabricated at the

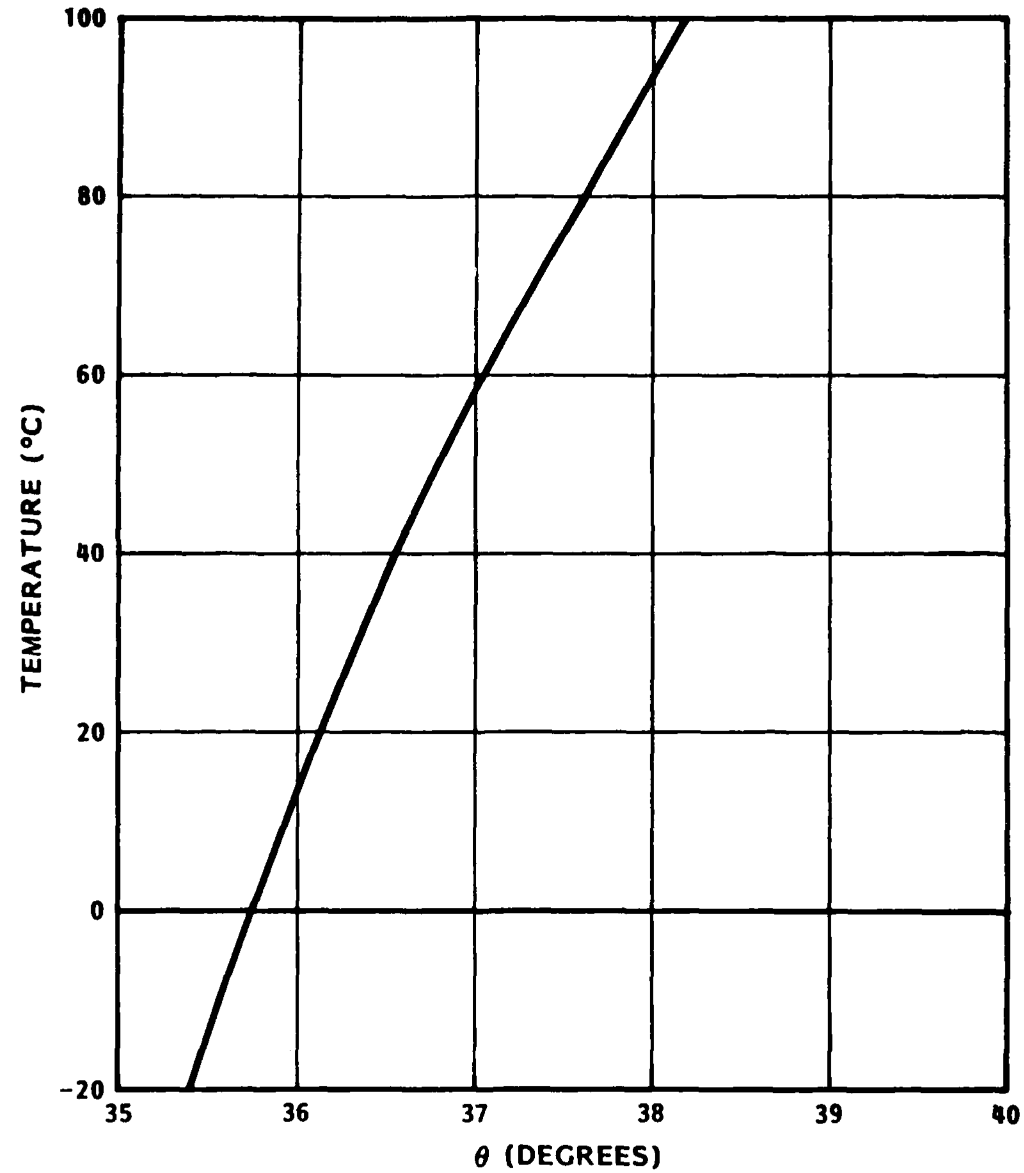

Figure 3-10. Turnover Temperature as a Function of Rotated Angle on Quartz with Aluminum Metallization ($H/\lambda = 0.015$)

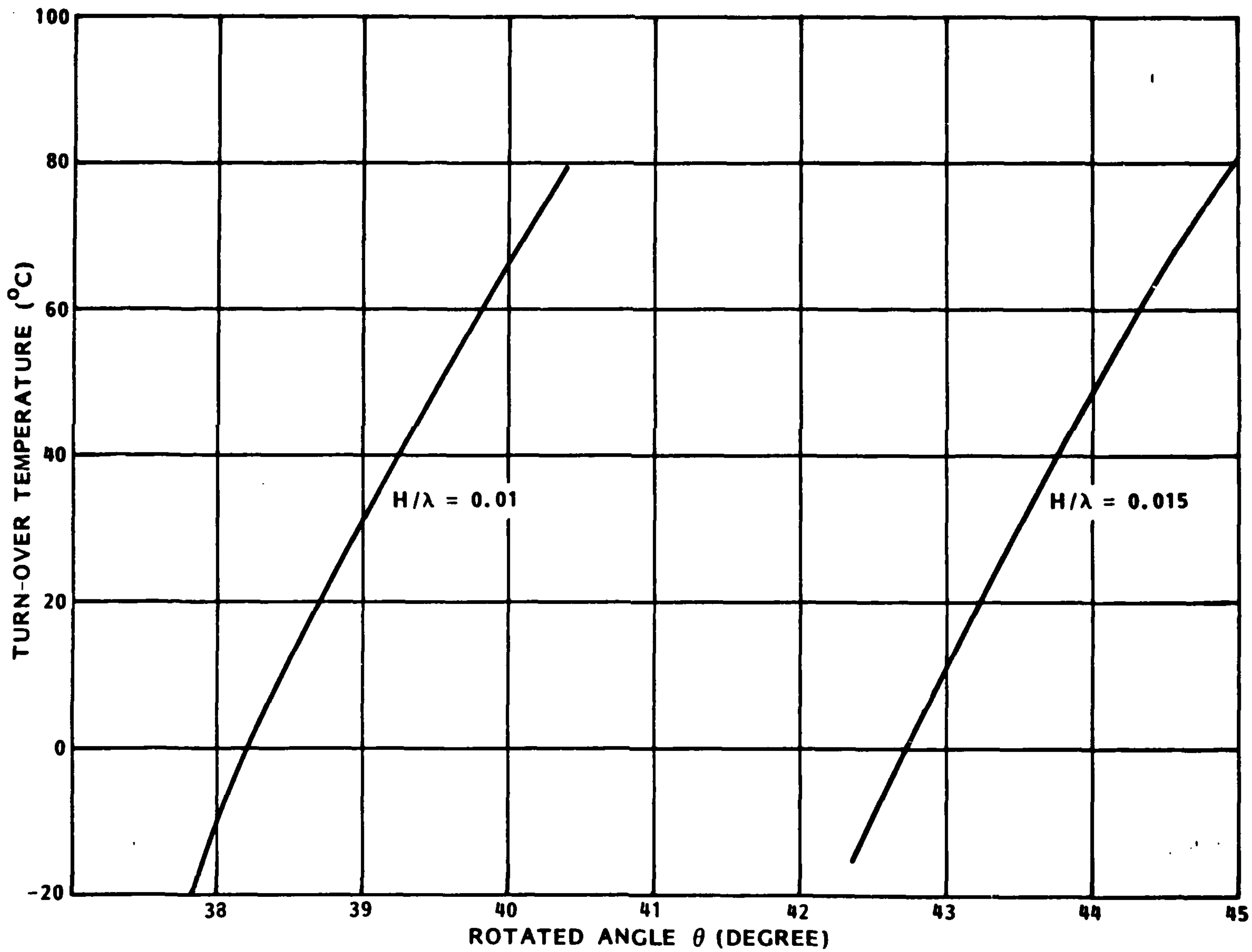

Figure 3-11. Turnover Temperature as a Function of Rotated Angle for Gold Metallization

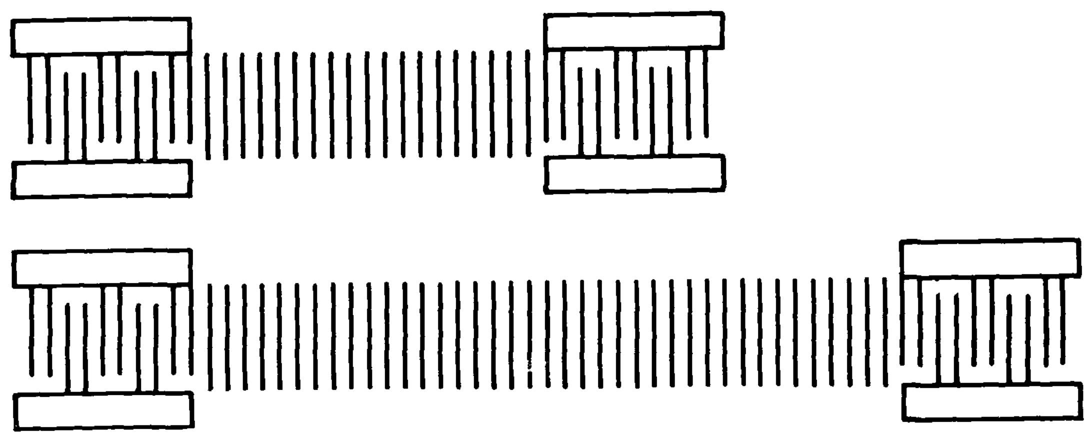

Figure 3-12. Experimental Arrangement for SBAW Propagation Loss Measurement

same time, any difference in insertion loss between the two devices can be attributed to the propagation loss.

Although the target frequencies of this program are 3 GHz, 5 GHz, and 10 GHz, the study was done at 1 GHz, which best utilized the low-cost photolithography process. Two trials at 1.04 GHz and $t/\lambda = 0.0115$ resulted in loss values of 8.7 and 9.3 dB/μsec. This result includes loss due to air loading, substrate surface condition and SBAW beam spreading.

Since the above result is so much higher than expected, an independent check was desired. Weglein and Otto[10] discussed a method of comparing the designed group delay τ_0 and the measured group delay τ_{eff} to obtain the propagation loss. The resulting equation is

$$\alpha \equiv \frac{6(1 - \tau_{eff}/\tau_0)}{\ell}$$

where α is the propagation loss, and ℓ the center to center separation of the transducers. Performing this calculation on existing data at 3.47 GHz, a loss of 97.7 dB/μsec is obtained, and 34.2 dB/μsec at 2 GHz, in good agreement with the values measured directly at 1 GHz. The two methods combined give the data in Figure 3-13. These data have some serious implications for device design in the GHz region. At 5 GHz, propagation loss would be on the order of 200 dB/μsec, which means devices must have fewer fingers, and transducers must be as close together as possible, consistent with minimizing electromagnetic feedthrough. Also, the plotted data roughly confirm the square-law dependence of propagation loss upon frequency.

Another point of interest is the fact that the same calculations applied to previously fabricated SAW oscillators indicate that SAW propagation losses are roughly a factor of 2 greater than SBAW losses at similar frequencies.

These data may also be compared to the results given above (3.1.2) for SBAW viscous material attenuation. It can be seen that the introduction of metal interdigital electrodes increases total propagation losses by roughly a factor of 5.

3.3 TRANSDUCER CONFIGURATION

Several types of transducer designs have been studied for SBAW devices at TRW. Since the thrust of this program is to construct stable SBAW

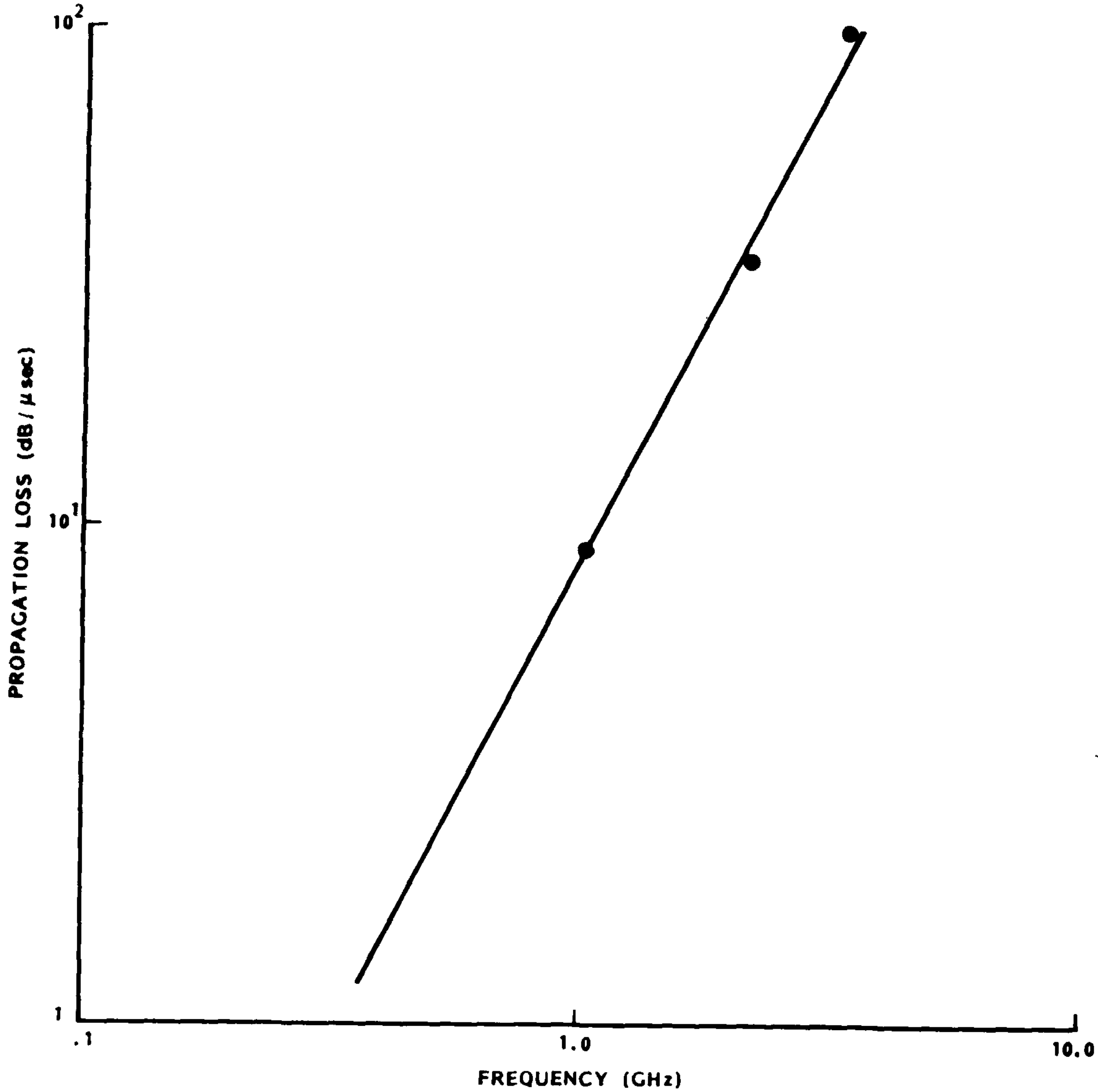

Figure 3-13. Propagation Loss as a Function of Frequency

oscillators at L through X-band, extensive studies were made on three types of transducer configurations. These include fundamental, fifth harmonic and seventh harmonic transducer configurations shown in Fig. 3-14.

The fundamental design employs two 2-finger/period (one up/one down) transducer configurations. The fifth harmonic design employs two 6-fingers/period (three up/three down) transducers. Both the fundamental and the fifth harmonic design use the primary response of the transducer which will be discussed in Section 3.4. The seventh harmonic device employs two 3-finger/period transducer configurations and operates at the secondary response. These transducer configurations allow construction of high Q, high frequency SBAW delay line oscillators.

3.4 HARMONIC OPERATION

Harmonic operation offers a method by which SBAW delay lines can be made to operate in the X-band region. This harmonic operation can be achieved with the use of a multi-electrode transducer configuration. The analysis of the harmonic operation is similar to that proposed by Engan[11] for SAW devices. Figure 3-15 summarizes the results of various multi-electrode configurations and their frequency responses. The finger width is assumed to be fixed, and only the primary and secondary responses are shown. The coupling strength of the secondary response is much weaker than the primary response and, although there are other higher order responses, their coupling strength is further reduced and has no practical application.

Figures 3-16 - 3-19 show the operating frequency of various multi-electrode transducers on rotated Y-cut quartz, assuming a fixed linewidth of 0.4 μm. The fundamental frequency of operation is denoted as F_0, and harmonics are expressed as $2F_0$, $3F_0$, etc. From these figures, it is seen that the maximum frequency of fundamental mode operation is around 3.2 GHz near AT-cut quartz. To obtain a higher frequency of operation with the 0.4 μm linewidth capability, one has to use harmonic operation of various multi-electrode transducers.

3.5 EQUIVALENT CIRCUIT MODEL

The theory of SBAW excitation and propagation on a free surface, developed at TRW, has provided a basis for modeling the time and frequency

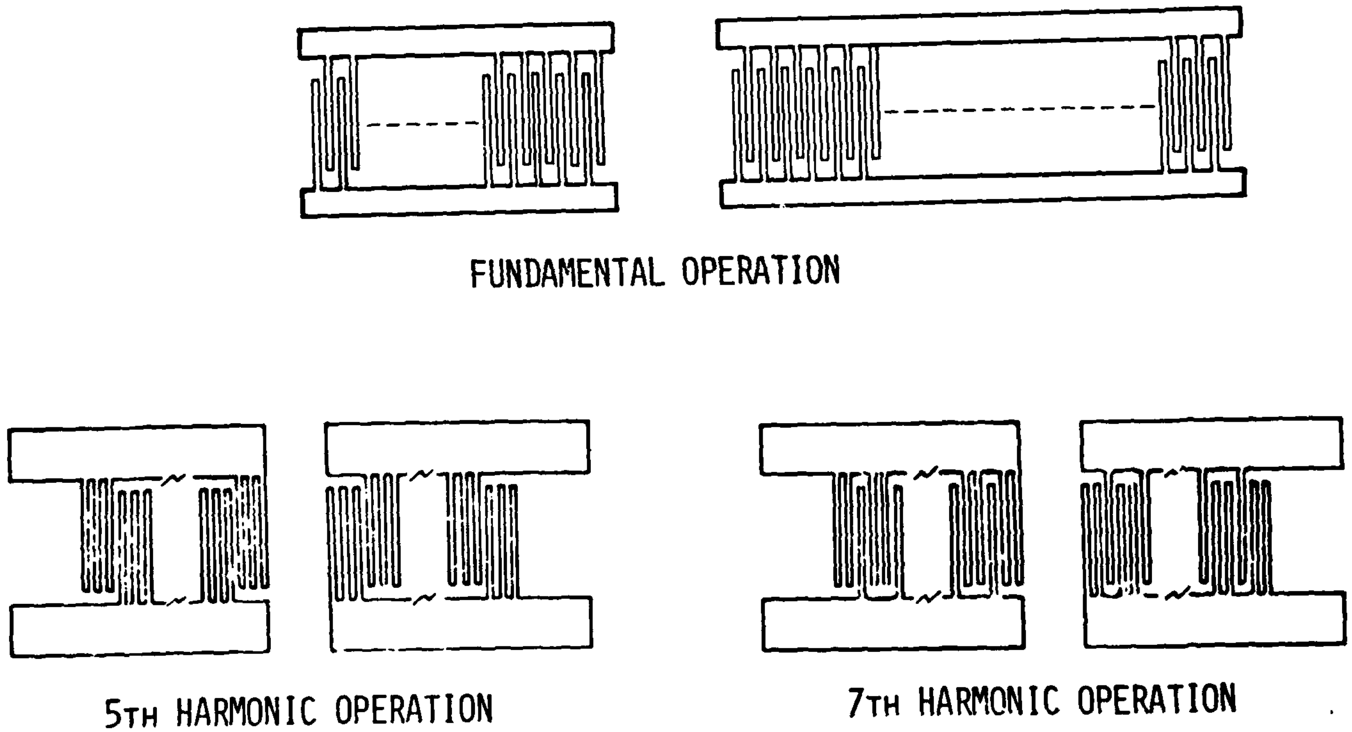

Figure 3-14. Transducer configuration for SBAW delay lines.

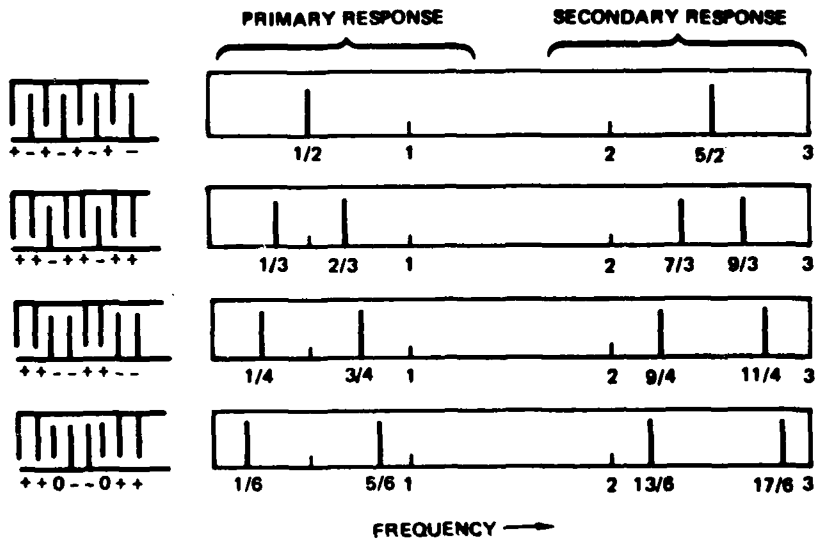

Figure 3-15. Transducer Configuration and Spectral Response (Fundamental and Harmonic Modes)

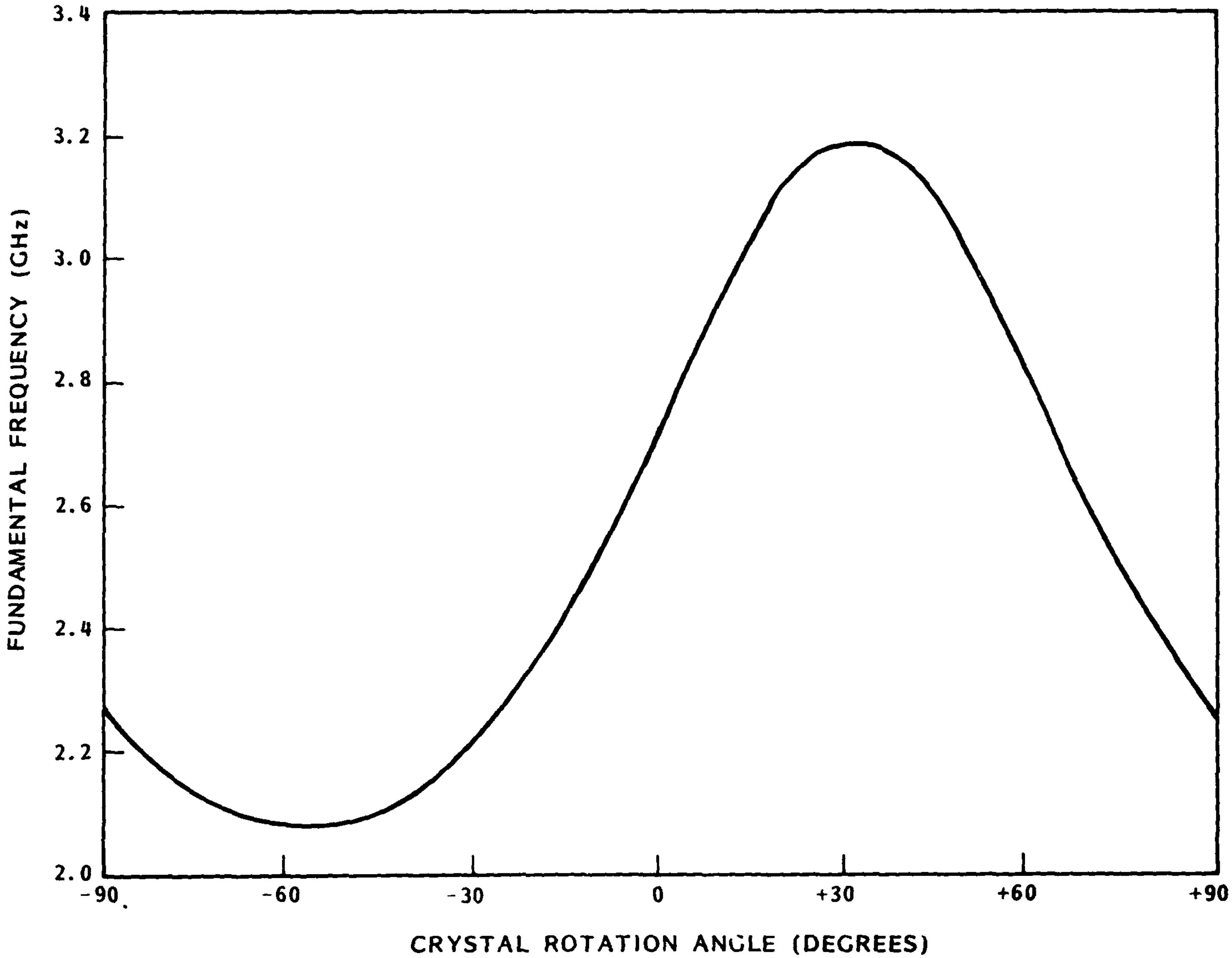

Figure 3-16. Fundamental Frequency as a Function of Rotated Angle on Quartz with 2 Fingers/Period Transducer Configuration (Linewidth = 0.4 μm)

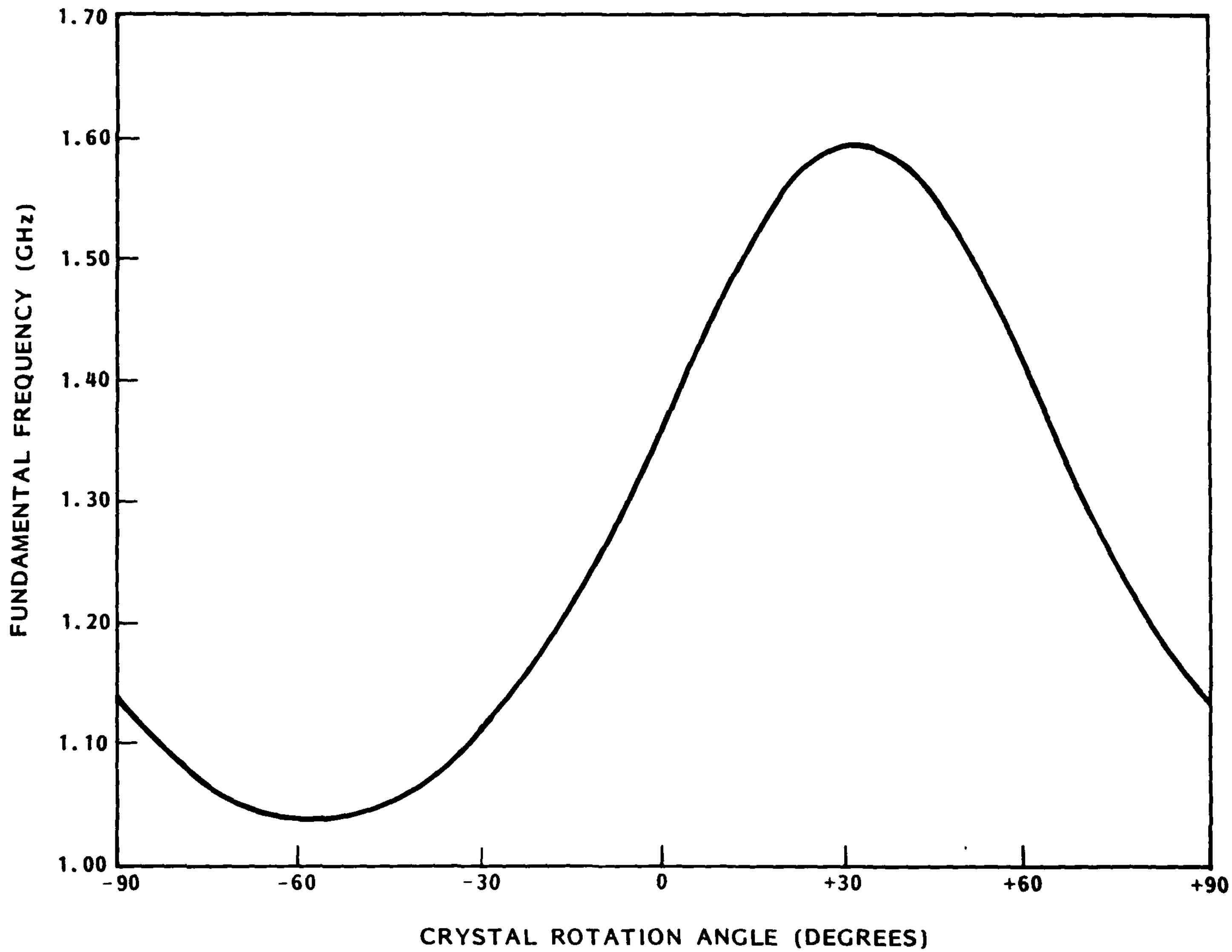

Figure 3-17. Fundamental Frequency as a Function of Rotated Angle on Quartz with 4 Fingers/Period Transducer Configuration (Linewidth = 0.4 μm). Harmonics exist at 3 F_o, 9 F_o, and 11 F_o.

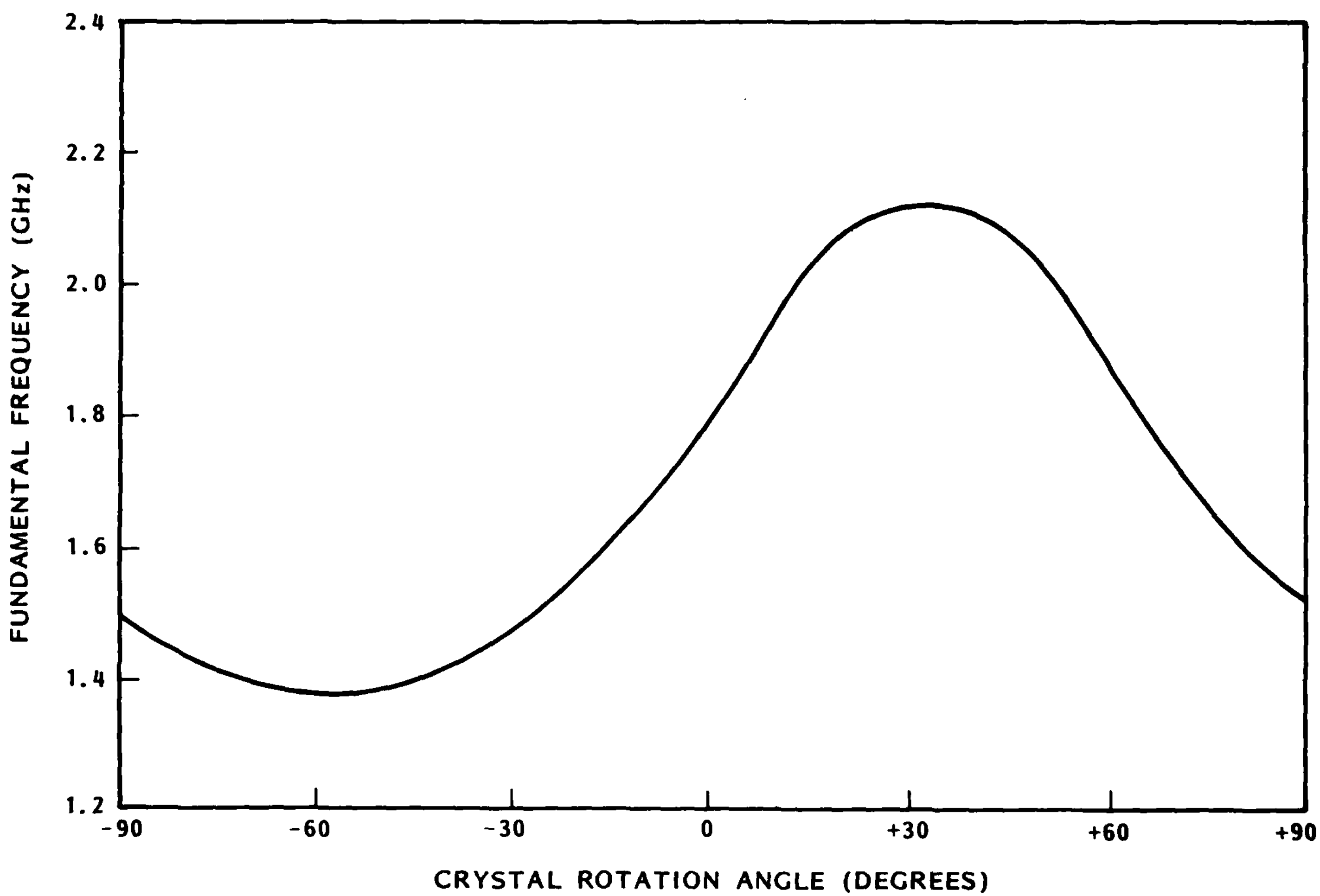

Figure 3-18. Fundamental Frequency as a Function of Rotated Angle on Quartz with 3 Fingers/Period Transducer Configuration (Linewidth = 0.÷ μm). Harmonics exist at 2 F_o, 7 F_o and 9 F_o.

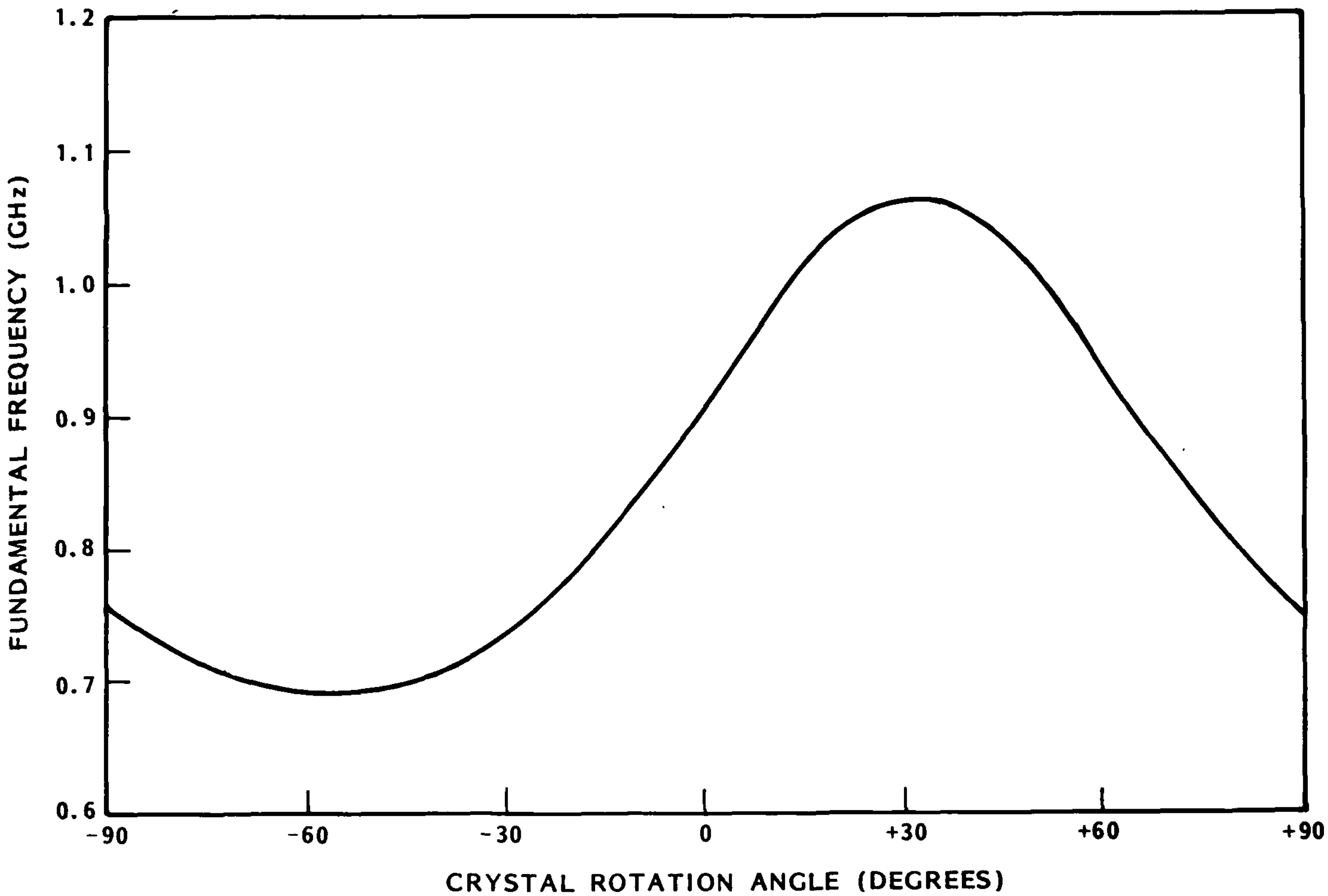

Figure 3-19. Fundamental Frequency as a Function of Rotated Angle on Quartz with 6 Fingers/Period Transducer Configuration (Linewidth = 0.4 μm). Harmonics exist at 5 F_o, 13 F_o, and 17 F_o.

domain responses of the SBAW delay lines. For practical purposes, the delta function model can be used in the modeling of the frequency response of high Q delay lines.

The piezoelectric coupling can be calculated using this model. Figure 3-20 shows the piezoelectric coupling constant, K_p^2, as a function of rotation angle.

The conversion loss of the transducer at the center frequency can also be calculated using the equivalent circuit model.[2] According to this model, the SBAW transducer at the center frequency is represented by radiation resistance in series with the capacitance C_T, as shown in Fig. 3-21. The insertion loss of the SBAW is the sum of four contributions: conversion loss of the input transducer, conversion loss of the output transducer, acoustic spreading loss given by

$$SL = 10 \log \frac{\lambda_C N}{4.5R} - 6 \text{ dB} \quad ,$$

and the propagation loss (discussed above). Table 3-2 uses this model in a loss factor analysis for a 3.1 GHz AT fundamental device fabricated under this program, and Table 3-3 shows the results for a 3.4 GHz device previously discussed in the literature.[2] In one case, the agreement is good, in the other, excellent. An AT 3.1 GHz device with 300 fewer fingers is analyzed in Table 3-4. Note that the agreement is a little better, and the predicted reduction in propagation loss appears largely responsible for the reduced insertion loss.

It appears that the TRW SBAW model, combined with the new propagation loss data, gives good agreement with experimental reality, and can serve as the basis for future device design.

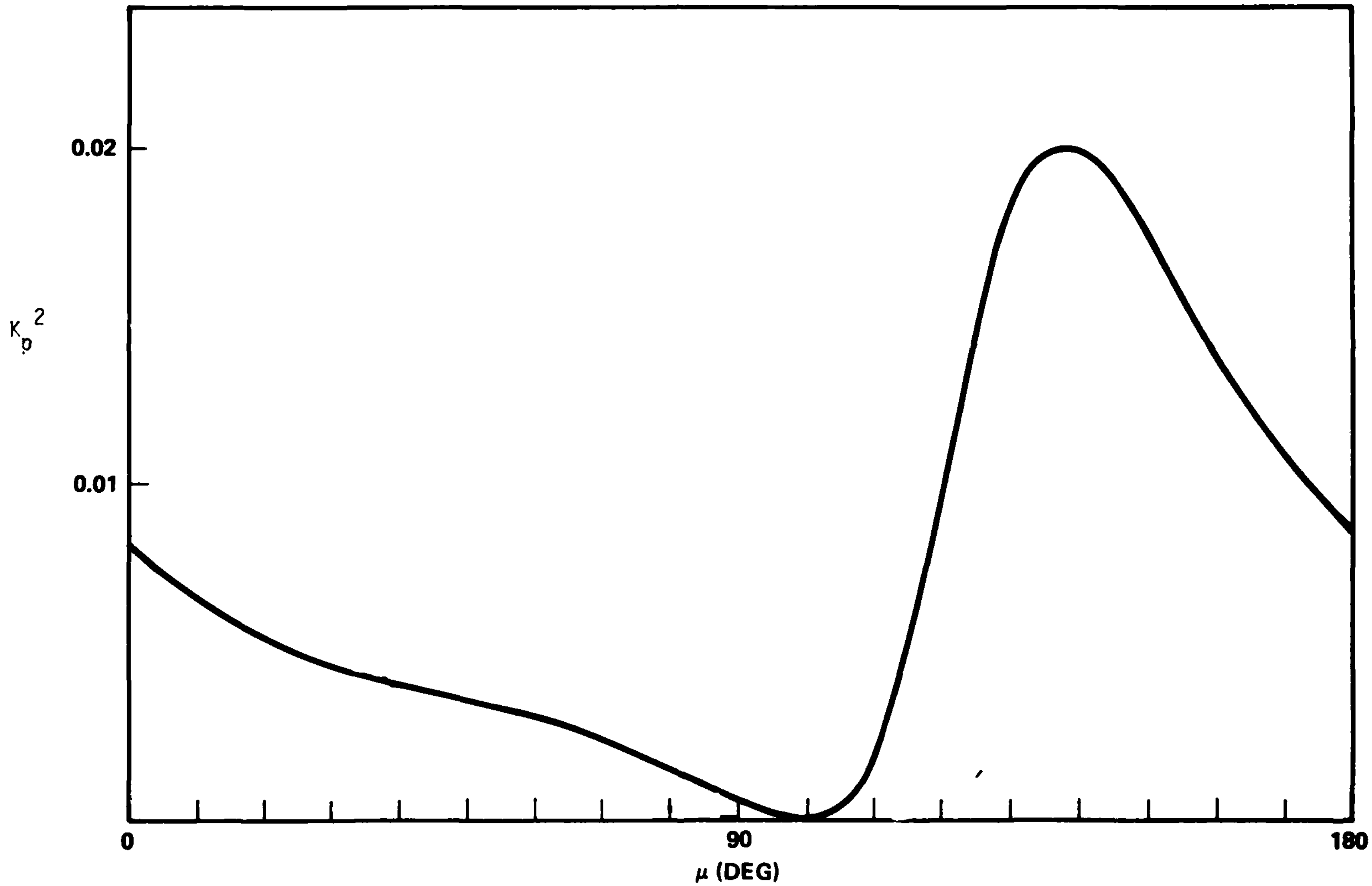

Figure 3-20. K_p^2 of SPAW in Rotated Y-Cut Quartz

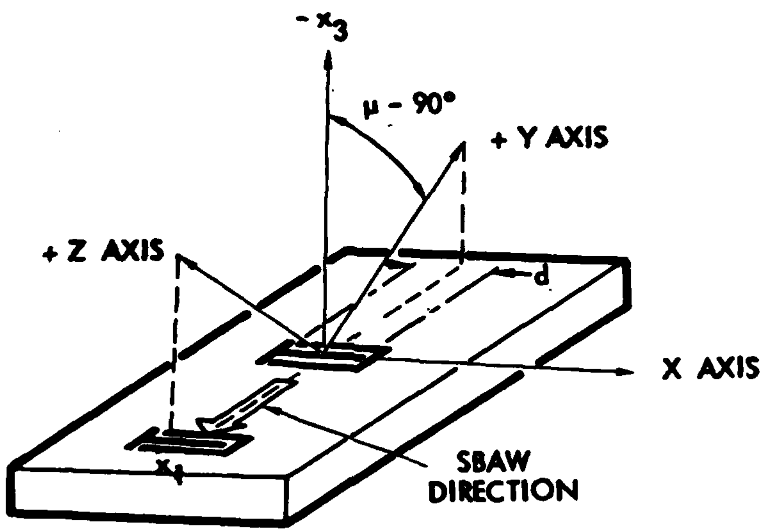

GEOMETRY OF A SBAW DEVICE
ON ROTATED Y-CUT QUARTZ

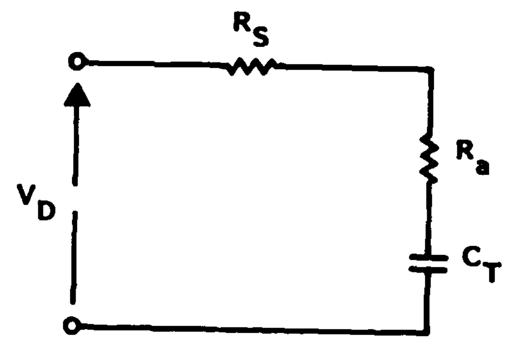

$$R_a \cong \frac{2}{\pi} \frac{1}{\sqrt{N}} K_p^2 \frac{1}{\omega_c C_s}$$

$$C_T = N\ C_s$$

$$I.L = C.L._1 + C.L._2 + S.L.$$

EQUIVALENT CIRCUIT MODEL
OF TRANSDUCERS

Figure 3-21. Equivalent Circuit Model for SBAW Transducers

Table 3-3. 3.1 GHz Loss Factor Analysis

(a) Device Parameters

Finger Width	0.4 μm
Gap Width	0.4 μm
Aperture Width	100 λ
Number of Fingers/Transducer	1001
Center-to-Center Separation of Transducers	1000 μm
Metallization	400 Å Al

(b) Loss Factors

Conversion Loss (Transducer 1)	10.3 dB
Conversion Loss (Transducer 2)	10.3 dB
Propagation Loss	14.2 dB
Resistor Loss	.7 dB
Spreading Loss	1.5 dB
Mismatch Loss (Transducer 1)	.2 dB
Mismatch Loss (Transducer 2)	.2 dB
Total	37.4 dB
Measured	34.0 dB

Table 3-4. 3.436 GHz Loss Factor Analysis

(a) Device Parameters

Finger Width	0.61	μm
Gap Width	0.61	μm
Aperture Width	75	λ
Number of Fingers/Transducer	201	
Center-to-Center Separation of Transducers	351	μm
Metallization	300	Å Al

(b) Loss Factors

Conversion Loss (Transducer 1)	4.7	dB
Conversion Loss (Transducer 2)	4.7	dB
Propagation Loss	6.2	dB
Resistor Loss	0.9	dB
Spreading Loss	2.1	dB
Mismatch Loss (Transducer 1)	1.6	dB
Mismatch Loss (Transducer 2)	1.7	dB
Total	21.9	dB
Measured	22.0	dB

Table 3-5. 3.1 GHz Loss Factor Analysis

(a) Device Parameters

Finger Width	0.4 μm
Gap Width	0.4 μm
Aperture Width	100 λ
Number of Fingers/Transducer	701
Center-to-Center Separation of Transducers	760 μm
Metallization	400 Å Al

(b) Loss Factors

Conversion Loss (Transducer 1)	9.6 dB
Conversion Loss (Transducer 2)	9.6 dB
Propagation Loss	10.8 dB
Resistor Loss	0.5 dB
Spreading Loss	1.8 dB
Mismatch Loss (Transducer 1)	.5 dB
Mismatch Loss (Transducer 2)	.7 dB
Total	33.2 dB
Measured	30.0 dB

4.0 SBAW DEVICE FABRICATION, MOUNTING AND PACKAGING

The manner in which SBAW devices are fabricated, mounted and packaged has a direct impact on device insertion loss, frequency reproducibility, and long-term aging characteristics. This section discusses the methods employed, and the results obtained.

4.1 CRYSTAL PREPARATION

Two types of quartz crystal have been employed: a relatively inexpensive electronic-grade, high Q quartz, and premium Q-swept quartz. The former is by no means an inferior grade of quartz--it is used in the production of TRW's flight-qualified SAW devices, and costs on the order of $40-50 per square inch. It is used in the various design iterations necessary for optimization. When a design is optimized, the premium Q-swept quartz is used. This material is grown in the Z plane; material growth in this plane is the purest. This high Q material shows unusually high stability in radiation environments. The material is synthetically grown and swept by Sawyer Research Products, and will be oriented within ± 10 minutes.

The substrates are cleaned with solvents to remove contamination and are then placed in uv/ozone after the methods of Vig, et al.[12] Once this is completed, the device is ready for further processing.

4.2 PHOTOLITHOGRAPHIC TECHNIQUES

Before photoresist is applied, a 30 Å flash of chrome or titanium is deposited on the quartz to promote photoresist adhesion. For devices with linewidths down to 0.6 μm, contact printing with a conformal mask and vacuum holder can be used. Devices in this category include the 7th harmonic, 9.9 GHz delay line and the 1680 MHz tunable oscillator. Recently, TRW installed a Karl Suss shallow uv contact mask aligner that can resolve linewidths down to 0.4 μm, and this system will replace the conformal mask and vacuum holder. In addition, a deep uv system (2200 Å radiation) is available for experimentation with PMMA resist.

Dark field masks are used to expose the patterns, which are then ion milled. Then, metal is deposited over the device, and the unwanted metal is lifted off. The critical step in the process is obtaining good contact between the mask and the photoresist. TRW has successfully applied this technique, using "regular" uv light, to fabricate devices with 0.5 μm linewidths.

4.3 ELECTRON BEAM FABRICATION

It is necessary to use e-beam exposure of resists to obtain the 0.4 μm linewidth necessary to fabricate oscillators with fundamental frequencies at 3.1 GHz because this resolution is presently beyond the capability of any mask fabricating facility that uses photolithography.

TRW's Cambridge EBMF-2 electron beam exposure system can be used either to fabricate devices using direct writing or to fabricate quartz masks. Efforts to date have concentrated primarily on direct writing of devices. Dark-field patterns are written in the PMMA resist, and a thin layer of metal (300-450 Å) is deposited on the surface. (The patterns are not embedded in the quartz because it was discovered the PMMA cannot withstand the ion milling. This will be discussed in greater detail in a later section.) The unwanted metal is then lifted off, and the metal fingers left on the surface. Figure 4-1 shows an excellent pattern on ST quartz fabricated with e-beam direct writing.

4.4 FABRICATION RESULTS

Fabrication efforts have focused on four major areas so far: 3.1 GHz fundamental frequency devices on AT quartz, 5 GHz 5th harmonic devices on AT quartz, 9.9 GHz 7th harmonic (secondary response) devices on AT quartz, and 3.5 GHz 5th harmonic devices on BT quartz.

4.4.1 5 GHz 5th Harmonic Devices on AT Quartz

The first devices designed and fabricated were the 5 GHz, 5th harmonic ones on AT quartz. The transducer configuration and design parameters are shown in Fig. 4-2. Original wafers had approximately 5500-6000 Å PMMA on the wafer, but exposure doses and development times were hard to optimize. It was decided to go to a thinner resist. Figures 4-3 and 4-4 show test patterns exposed and developed in 3000 Å of PMMA on a silicon wafer. The lithography was excellent, so resist thicknesses in this range have been used. Thinner resists have not been attempted because of the necessity of getting clean liftoff of the unwanted metal.

Figures 4-5 - 4-7 show responses of a 5 GHz, 5th harmonic delay line on AT quartz. As can be seen, the response at the desired frequency is less than satisfactory. One explanation is that the PMMA does not appear to successfully withstand the ion milling process step. Comparison of

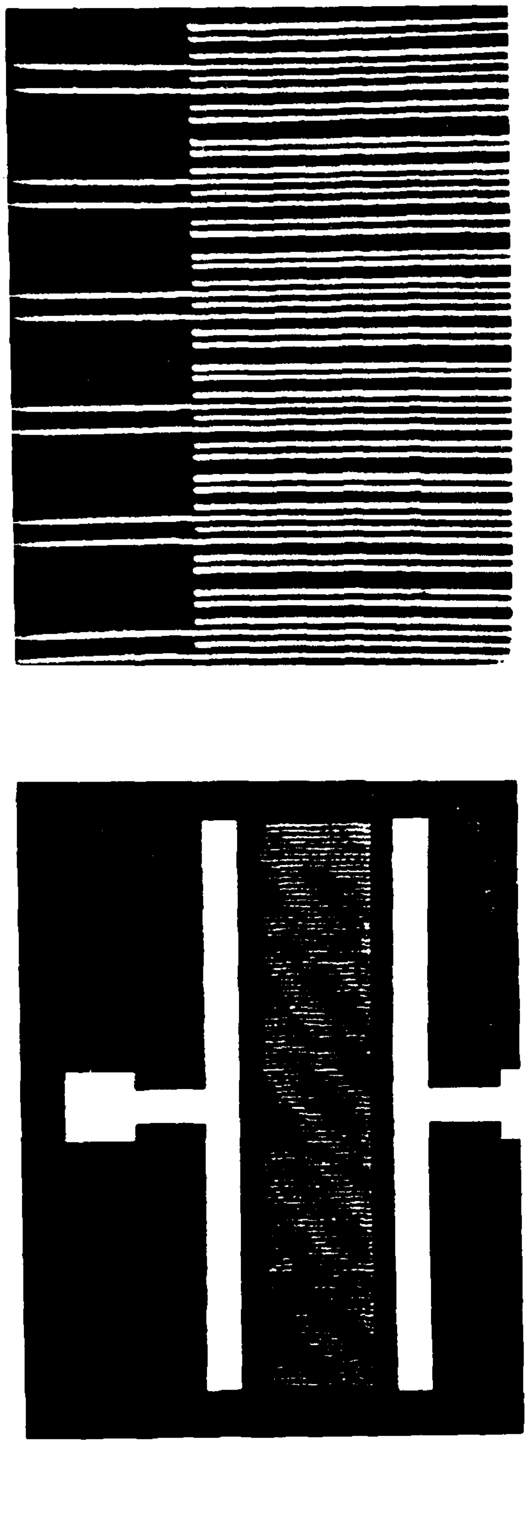

Figure 4-1. E-Beam Fabrication of SRAW Delay Line (Finger Width = Gap Width = 0.4 μm)

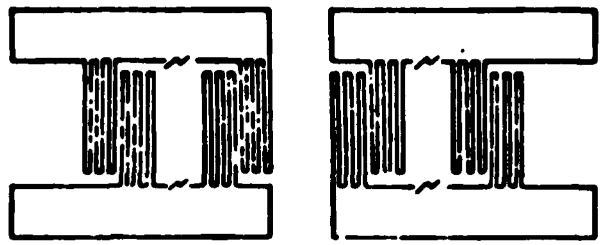

(a) Transducer Configuration

Finger Width	0.4 μm
Gap Width	0.4 μm
No. of Fingers (3 up, 3 down)	531
Aperture Width	132 μm
Center-to-center Separation Between Transducers	474.4 μm
Oscillator Q	1400

(b) Design Parameters

Figure 4-2. Low-Q 5th Harmonic Delay Line

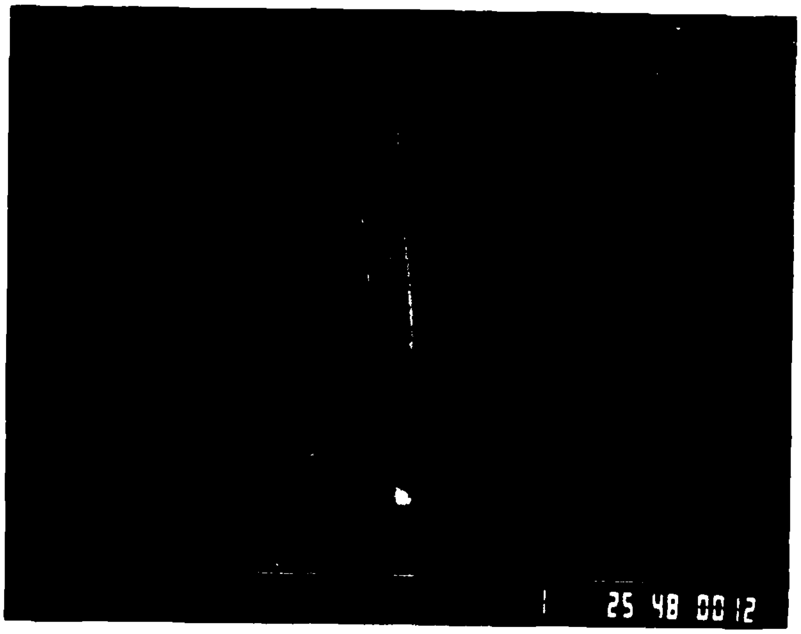

Figure 4-3. 3K Å PMMA on Silicon, 10000X

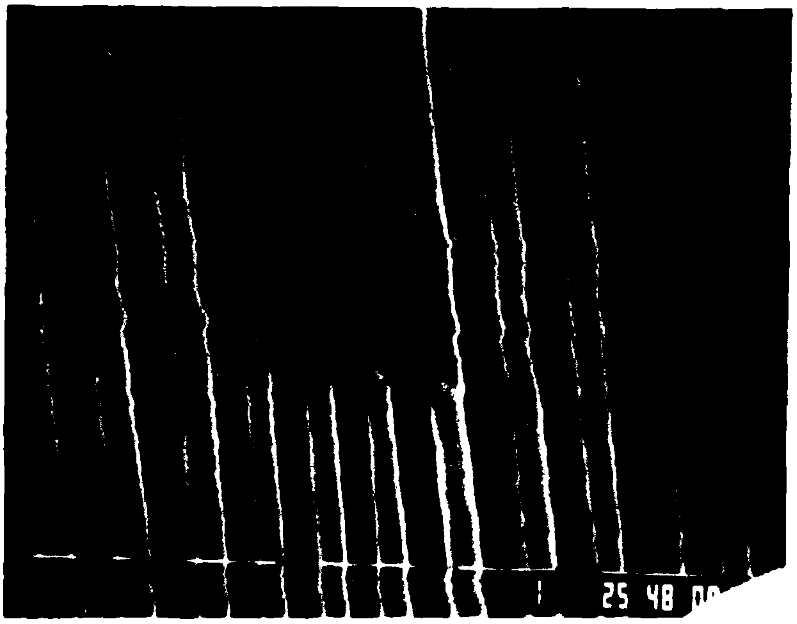

Figure 4-4. 3K Å PMMA on Silicon, 15000X

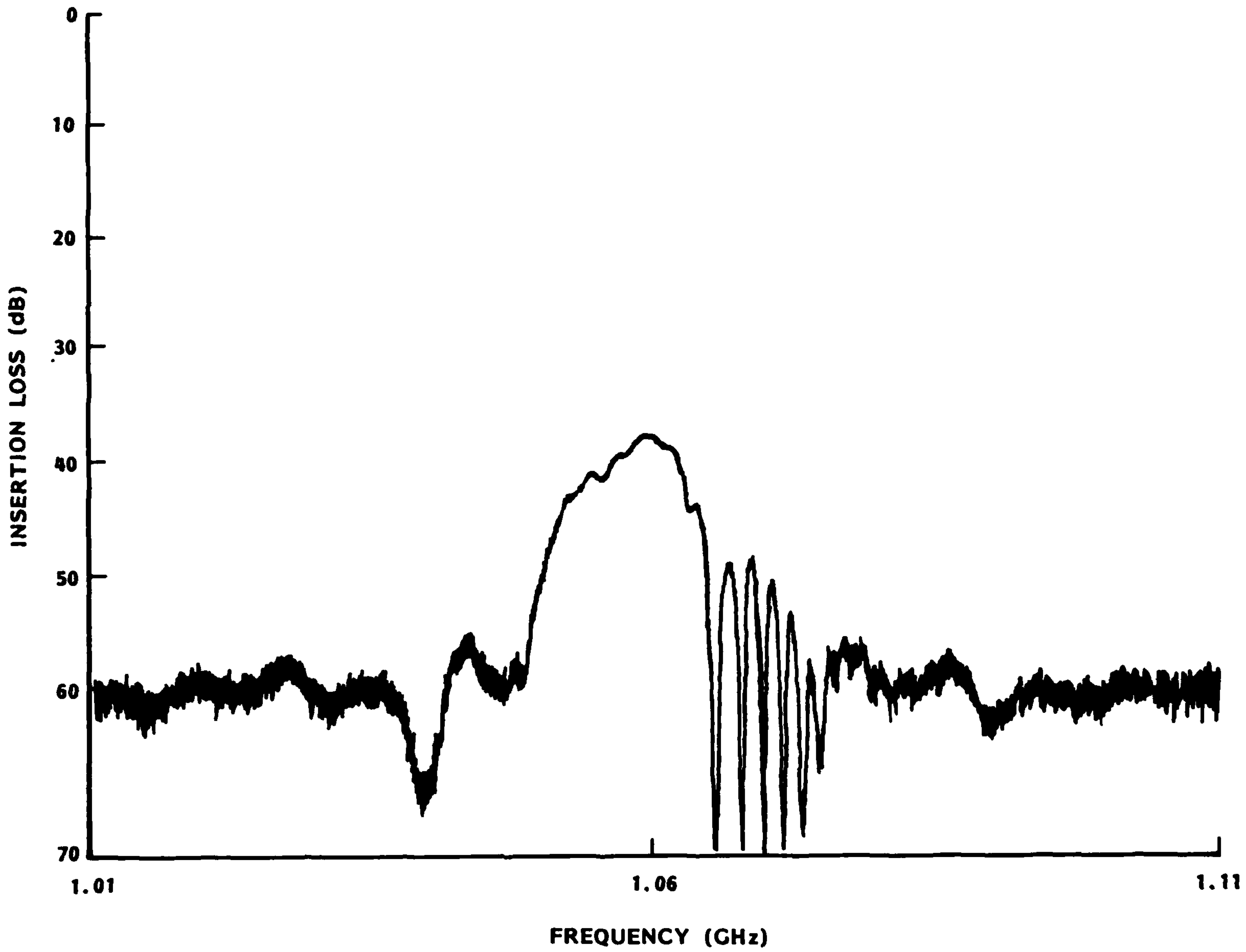

Figure 4-5. Fundamental Response of 5 GHz SBAW Device

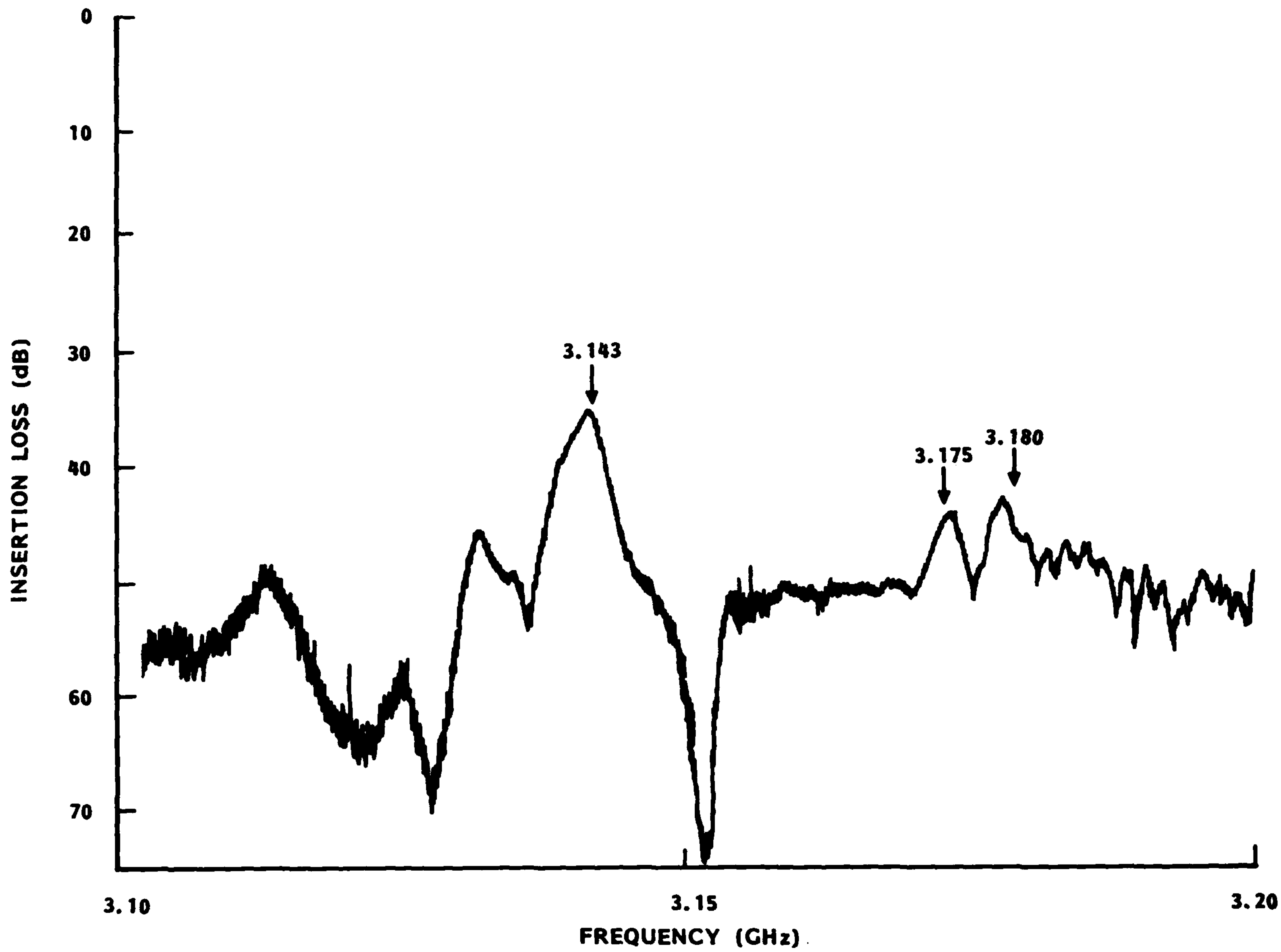

Figure 4-6. Third-Harmonic Response of 5 GHz SBAW Device

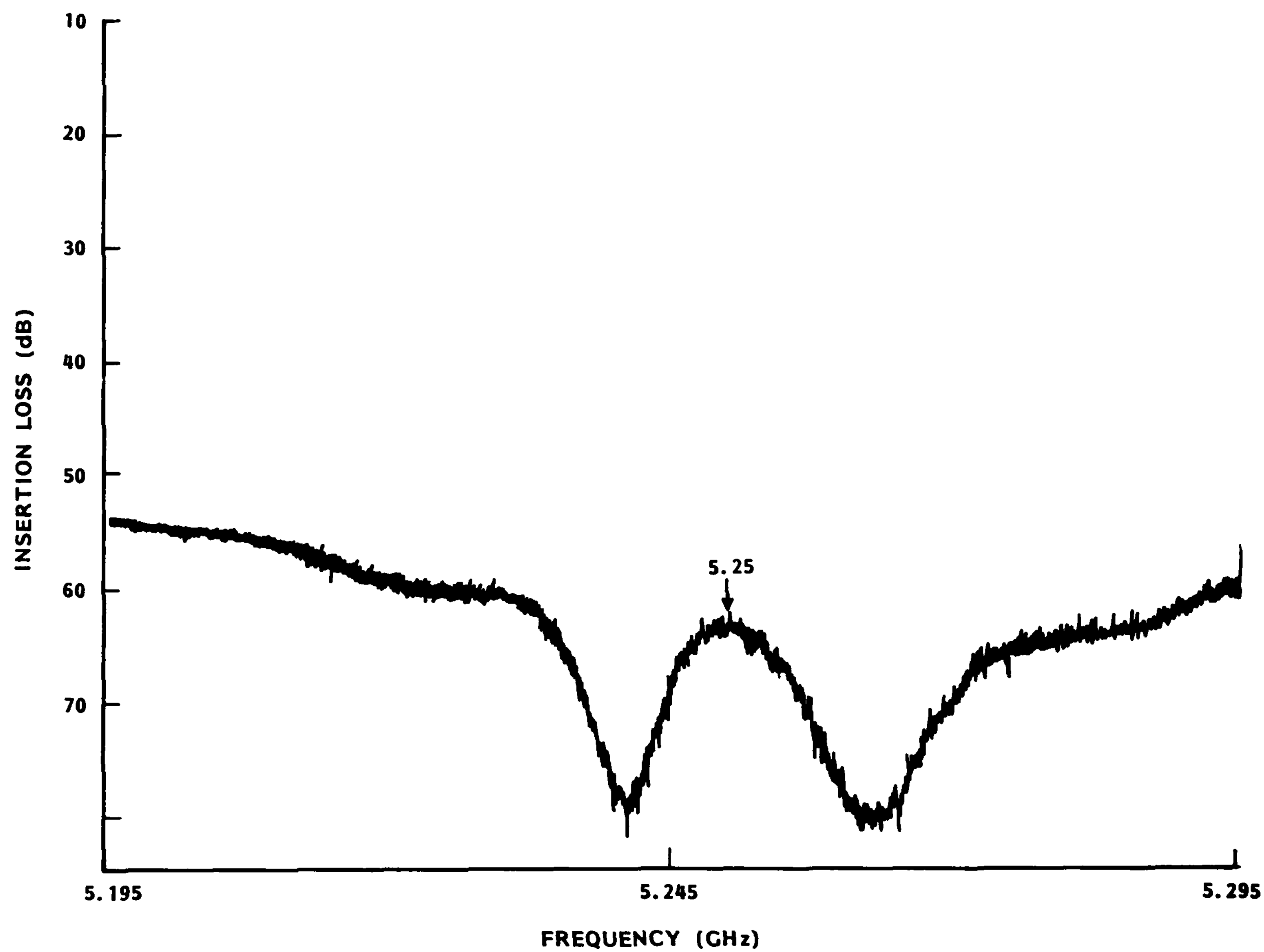

Figure 4-7. Fifth-Harmonic Response of 5 GHz SBAW Device

"before" and "after" photographs distinctly show degradation of the resist profile and what appears to be some deformation or flow of the lines of resist. Liftoff becomes more difficult and usually is not totally accomplished, which leaves metal bridges at many places on the device.

The conclusion was reached that PMMA cannot be ion milled, and embedding the transducers required another approach. Several avenues of exploration have been considered. The first involves a two-level resist, shown schematically in Fig. 4-8. The PC-120 resist used at TRW is also sensitive to e-beam exposure, and withstands the ion milling better than PMMA.

After the PC-120 is exposed and developed (b), the device is ion-milled through the Ti, which is then used as a mask for ion-milling through the PMMA and into the quartz. Another possibility is to avoid ion-milling, or to simply deposit aluminum on the surface of the quartz without embedding it. For harmonic operation, embedding is necessary, so depositing the metal on the surface is not an option here.

A new option is using the e-beam machine to expose a quartz mask, and then use the new Karl Suss mask aligner to replicate the patterns in a standard Shipley resist, which withstands ion milling well. This is currently under development.

4.4.2 3.5 GHz 5th Harmonic Devices on BT Quartz

It was realized recently[13] that it is probably not necessary to embed high-frequency devices on BT quartz. The fact that the SBAW velocity in BT quartz and aluminum is very similar makes this possible, but the frequency of operation is lower. SBAW velocity in AT quartz is 5100 m/sec, but is only 3300 m/sec in BT quartz. Thus, the same device design mentioned earlier that yields a 5 GHz device on AT quartz gives a 3.5 GHz device on BT quartz. In addition, propagation loss on BT quartz is not thought to be as large, so the number of fingers can be increased a great deal, raising the Q and narrowing the bandwidth. Of course, as the number of fingers increases, so, too, will the propagation loss, and a point is reached where adding fingers increases the insertion loss. Therefore, all designs have an excessive number of fingers based on the reasoning that the number of fingers may be decreased but not increased after fabrication.

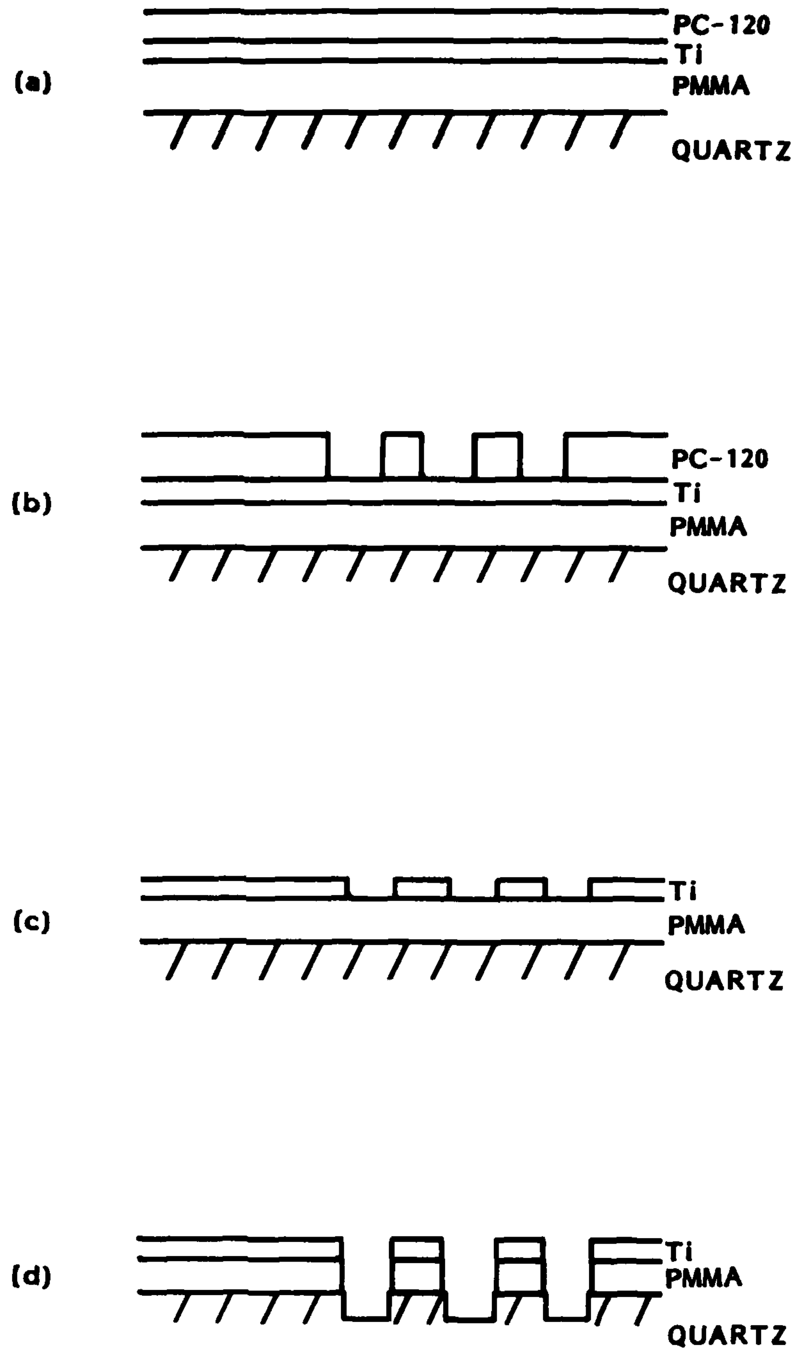

Figure 4-8. Schematic of Two-Level Resist Process Step

Another significant advantage of using BT quartz is its lower temperature coefficient. The device design is shown in Figure 4-9. The design has an aperture width of 75 wavelengths of interest.

Figure 4-10 shows an untuned device of this design. Tuned, it had an insertion loss of 42 dB. This particular device had 60% of its fingers removed by laser trimming, and had the best response of the lot. That suggests that perhaps the design had too many fingers, even for BT quartz.

It was thought that other apertures should be checked, so two new devices were designed, identical to the one shown in Figure 4-9, except that one had an aperture of 50 λ, and the other an aperture of 100 λ. A test result from a 50 λ aperture device is shown in Figure 4-11. Tests have not yet been made on the 100 λ devices.

4.4.3 3.1 GHz Fundamental Devices on AT Quartz

It is believed that embedding of transducers is not critical for fundamental mode, one-up-one-down finger patterns. Therefore, these devices have used e-beam exposure of PMMA, but no ion milling. The metal is deposited directly on the surface. The device design is shown in Figure 4-12, and test results are shown in Figures 4-13 and 4-14.

Since the devices on BT quartz appeared to have too many fingers, it was thought that this design might have a similar problem. The device in Fig. 4-15 had 30% of its fingers clipped, and the device in Figure 4-16 had 50% cut. Note the progressive deterioration of the wave form--a stop band was created. This is probably due to the method of trimming fingers. They are cut near the transducer, but not totally removed. It is believed that reflections from the trimmed fingers formed a low Q resonator and distorted the wave form, and that if the fingers had been totally removed, the insertion loss would have improved more. Therefore, a new design was done with a reduced number of fingers, shown in Figure 4-17. These are currently being tested.

4.4.4 9.9 GHz 7th Harmonic Devices on AT Quartz

A 7th harmonic, 9.9 GHz device was designed with the parameters shown in Fig. 4-18, to be replicated as devices using a Shipley resist on AT quartz, followed by ion milling and metal deposition.

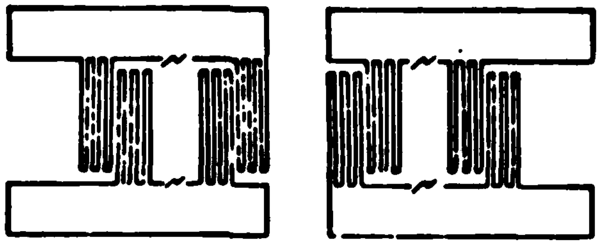

(a) Transducer Configuration

Finger Width	0.4 μm
Gap Width	0.4 μm
No. of Fingers (3 up, 3 down)	1023
Aperture Width	132 μm
Center-to-Center Separation Between Transducers	868 μm
Oscillator Q	2800

(b) Design Parameters

Figure 4-9. High-Q 5th Harmonic Delay Line

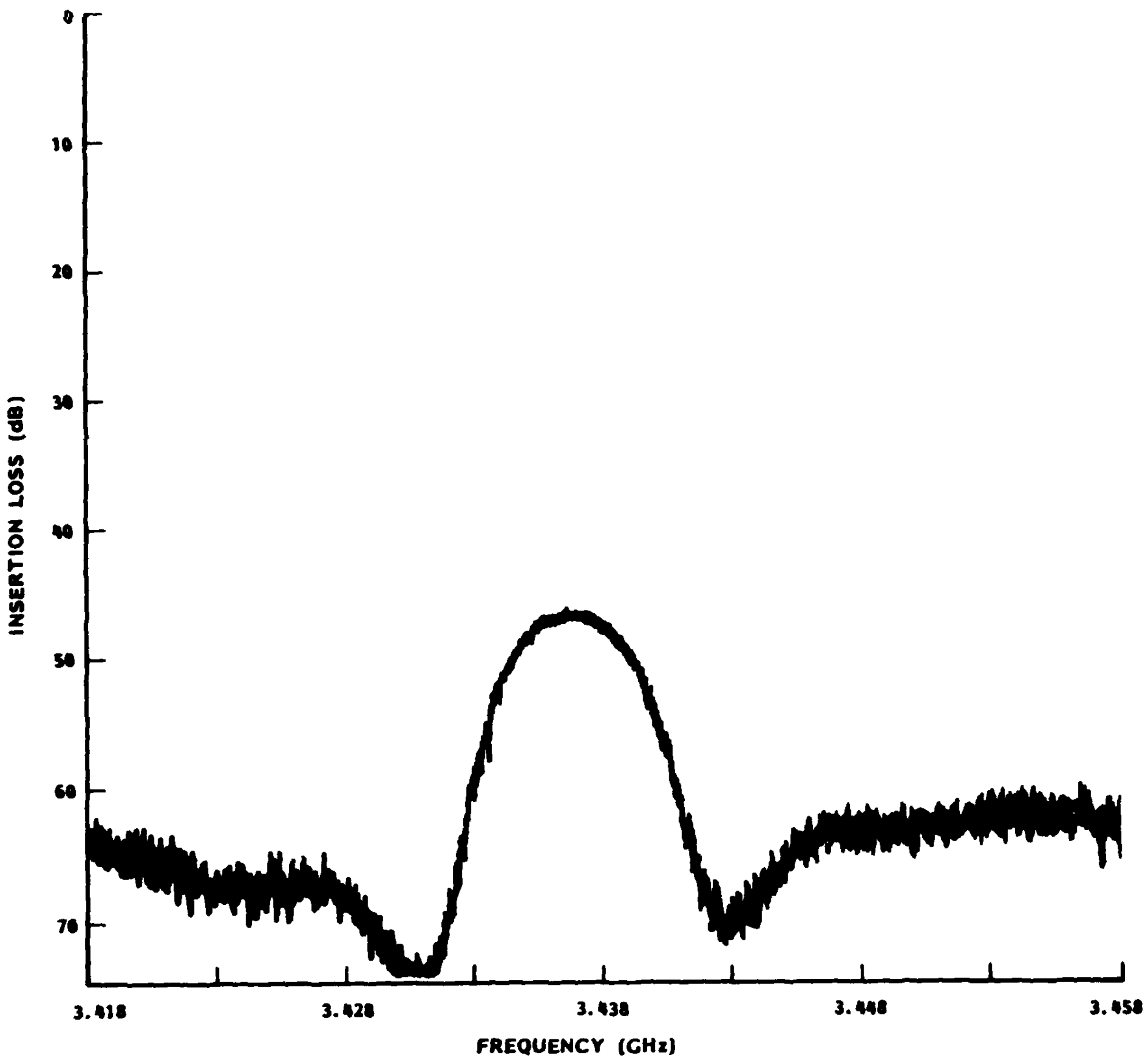

Figure 4-10. 3.5 GHz Fifth-Harmonic Device on BT-Cut Quartz

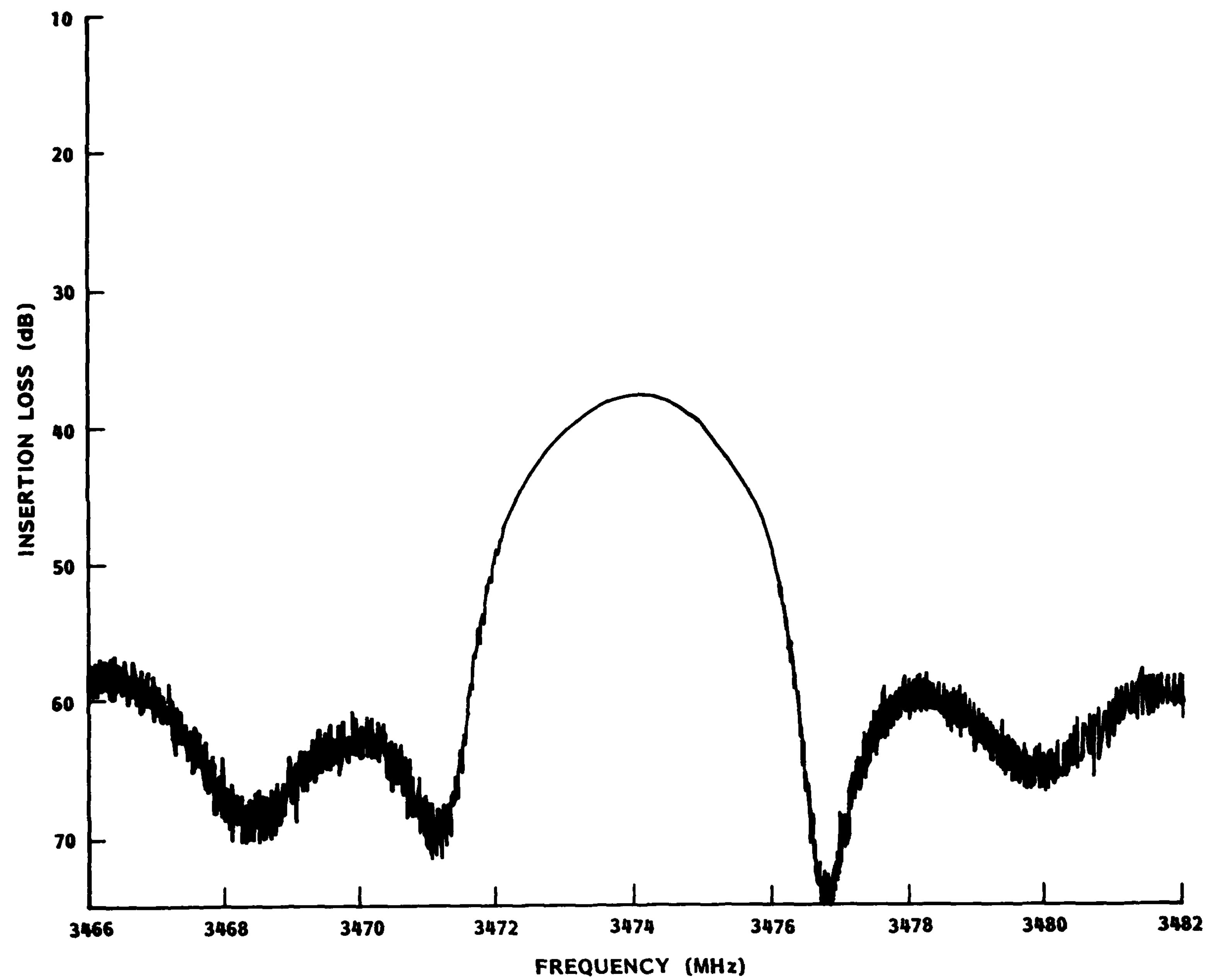

Figure 4-11. Fifth-Harmonic SBAW Device on BT-Cut Quartz

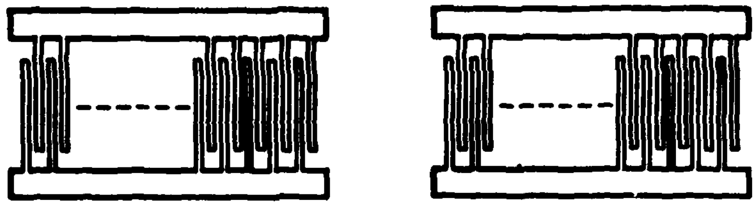

Finger Width	0.4 μm
Gap Width	0.4 μm
Aperture Width	100 λ
Number of Fingers/Transducer	1001
Center-to-Center Separation of Transducers	1000 μm
Distance Between Transducers	200 μm

Figure 4-12. 3 GHz Fundamental Delay Line

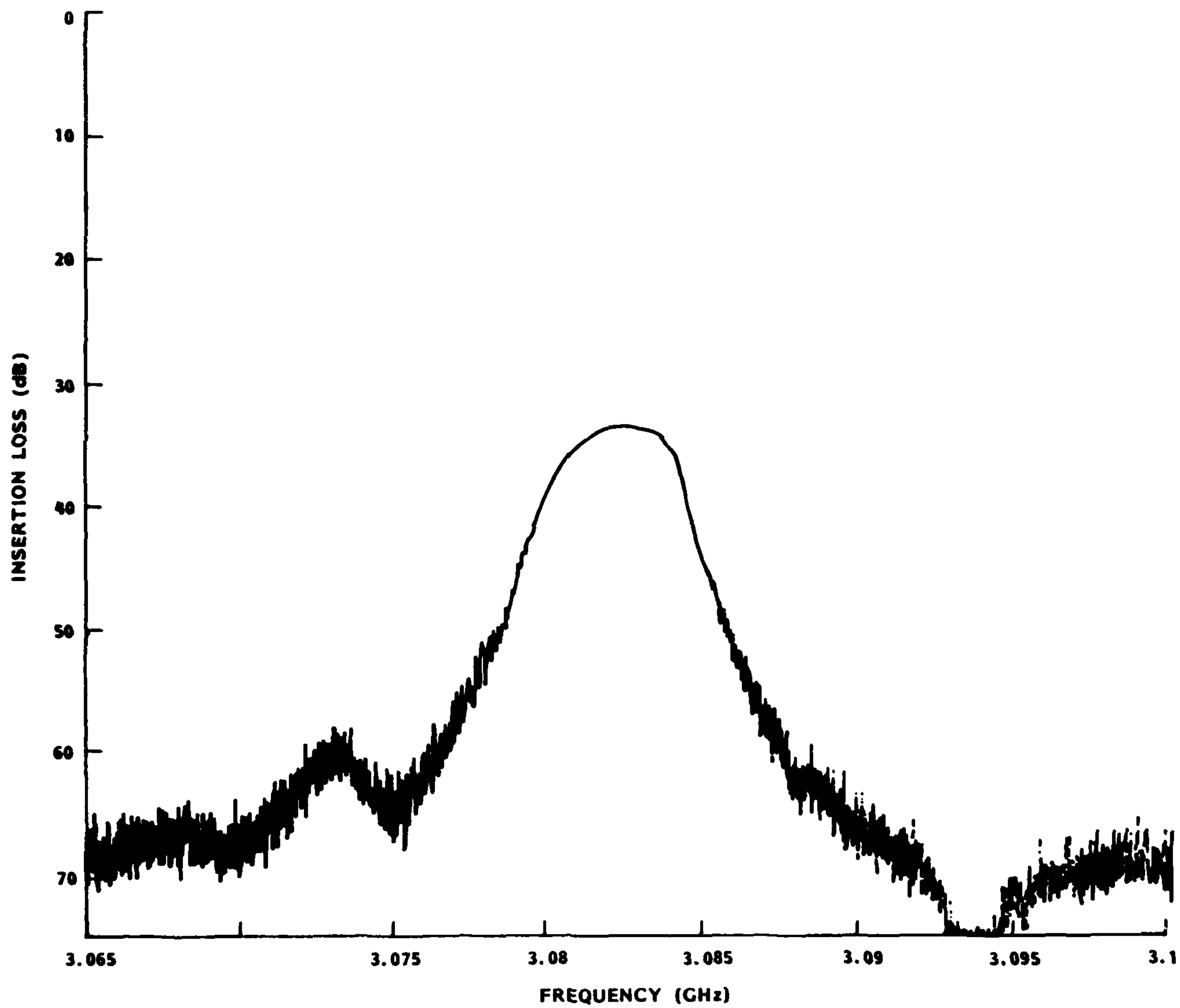

Figure 4-13. 3 GHz Fundamental Mode Response of SBAW Device (Untuned)

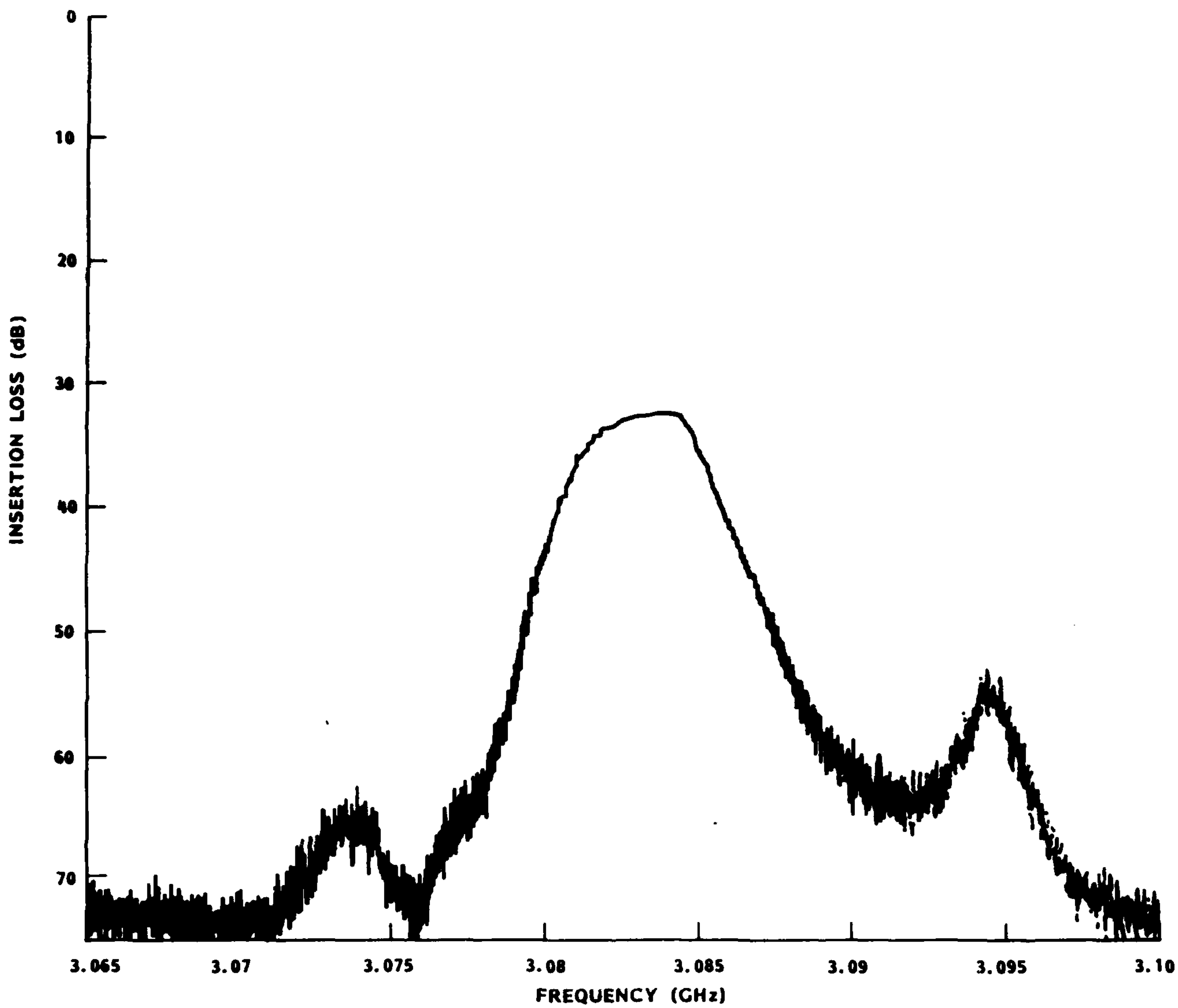

Figure 4-14. 3 GHz Fundamental Mode Response of SBAW Device (Tuned)

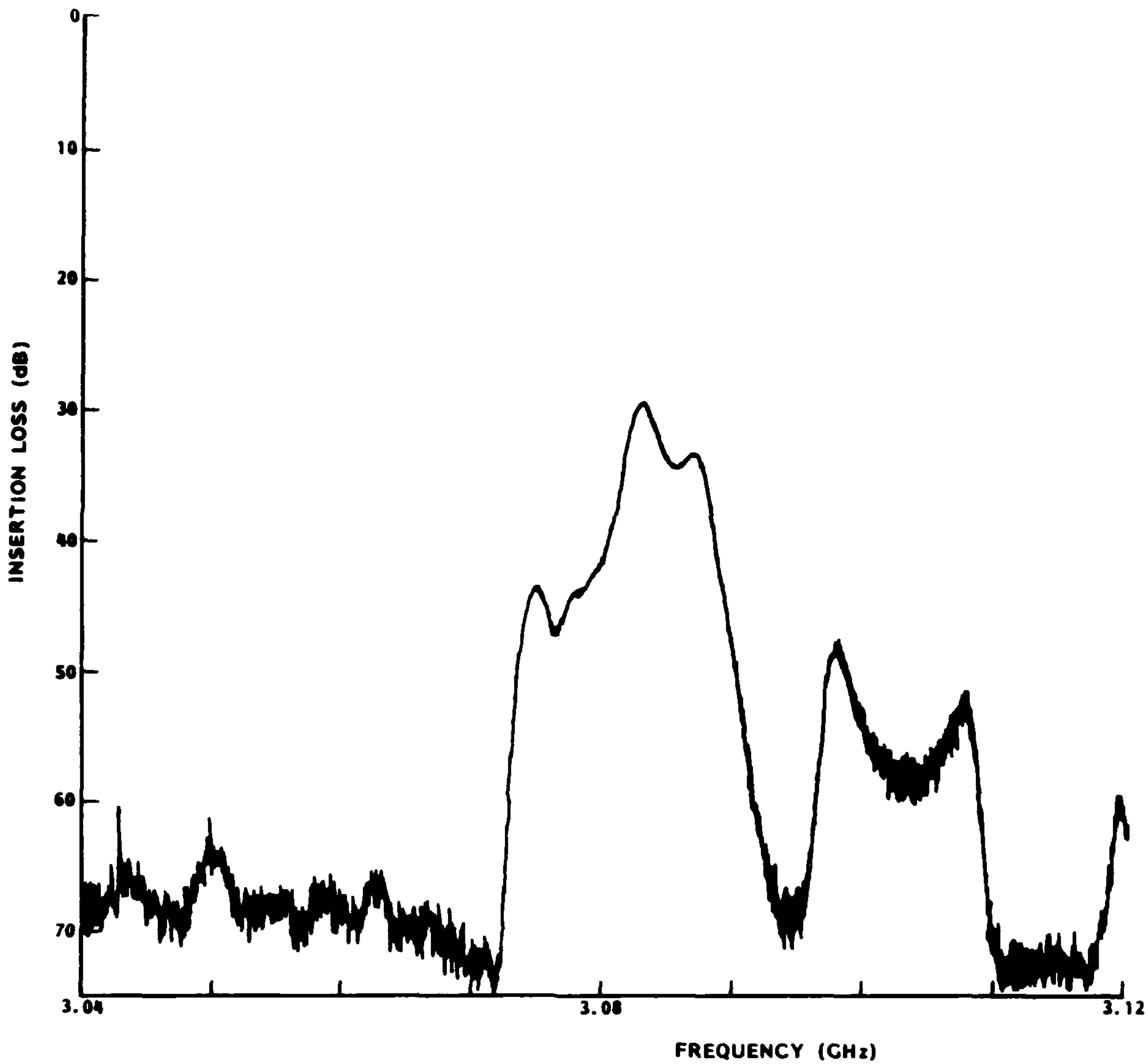

Figure 4-15. 3 GHz Fundamental Mode Response of SBAW Device

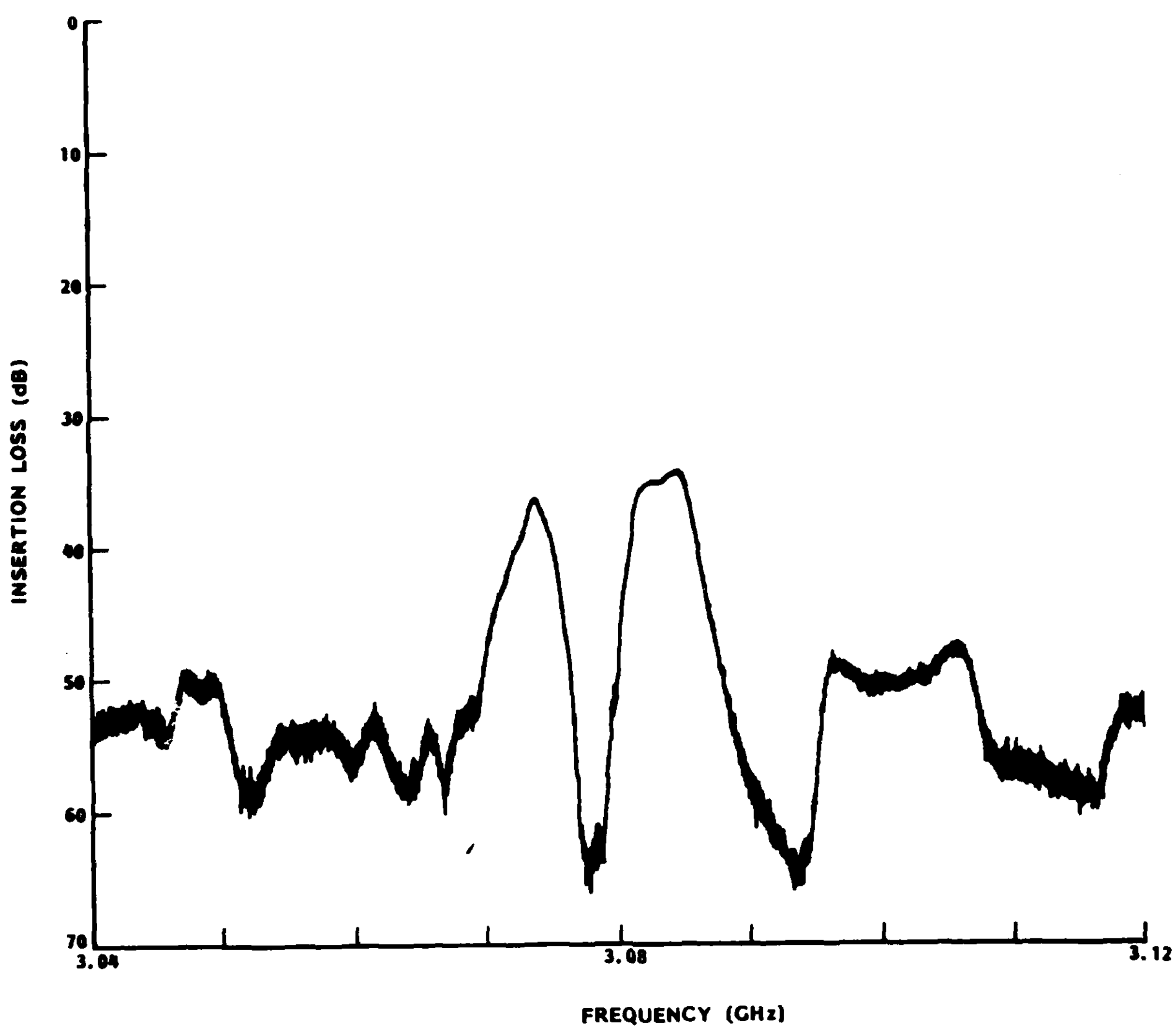

Figure 4-16. 3 GHz Fundamental Mode Response of SBAW Device

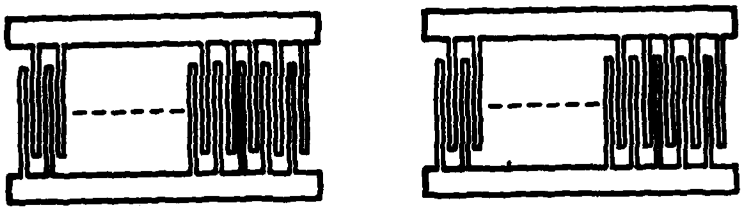

Finger Width	0.4 μm
Gap Width	0.4 μm
Aperture Width	80 λ
Number of Fingers/Transducer	501
Center-to-Center Separation of Transducers	450.4 μm
Distance Between Transducers	50 μm

Figure 4-17. 3.1 GHz Fundamental Delay Line

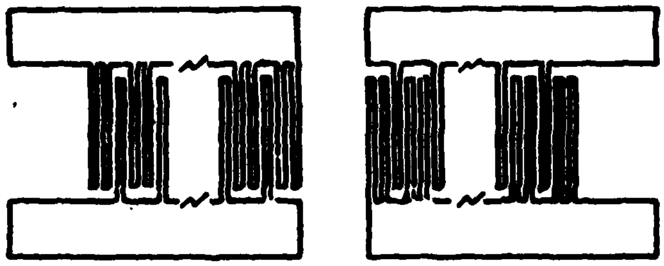

Finger Width	0.6 μm
Number of Fingers/Transducer	188
Aperture Width	40 μm
Center-to-Center Separation of Transducers	255 μm
Distance Between Transducers	30 μm

Figure 4-18. 9.9 GHz SBAW Delay Line

4.5 MOUNTING AND PACKAGING

The device mounting and packaging is expected to greatly affect the aging characteristics of the SBAW device. The four-pin HC-37 can with electrodeless nickel plating is the preferred package in which to mount the SBAW crystals in order to ensure the highest cleanliness while still satisfying the vibration requirements. Figure 4-19 illustrates how the SBAW delay line will be mounted. A stainless-steel clip (not shown in the picture) will be used to keep the device in place, eliminating the need for RTV, and thus improving the aging of the device.

Direct electromagnetic feedthrough is always a problem at high frequencies, and was checked for this package. Figure 4-20 shows the feedthrough between 2 and 3 GHz. At 3 GHz, the feedthrough level is already -25 dB, which would drown any of the devices fabricated to date. Another possible package examined was the ceramic flatpack developed by Filler.[14] The electromagnetic feedthrough of this package is shown in Fig. 4-21. This package is significantly better overall, but still not good enough, so the HC-37 can was studied to see if it could be improved. The leads inside and outside the package were shortened and the device was grounded directly to the package, and feedthrough was reduced to -45 dB from 2.0 to 3.5 GHz, rising to -40 dB at 5 GHz. A metal sheet placed inside the can on top of the delay line should suppress feedthrough by at least 50 dB from 2 to 4 GHz, and 45 dB from 4 to 5 GHz.

Another method to reduce feedthrough uses an overlay mask to build up and lengthen the electrodes on the quartz, so as to reduce the length of aluminum bonding wire necessary to reach from the pins to the device, thereby reducing the antenna radiation of the bond wires. Current devices are being fabricated with this new process step added, which is expected to suppress feedthrough another 3-5 dB. Therefore, the HC-37 package will be satisfactory.

The package will be hermetically sealed at 10^{-9} torr using the cold welder shown in Figure 4-22. This cold welder has the particular feature of combining analytical tools, such as an Auger electron spectrometer and a mass spectrometer into the same chamber as the cold welder sealer. The SBAW device can be analyzed for surface cleanliness and monitored for specific contaminants before the device is placed in the cold welder and sealed.

Figure 4-19. Proposed SBAW Delay Line Package (HC-37 Can)

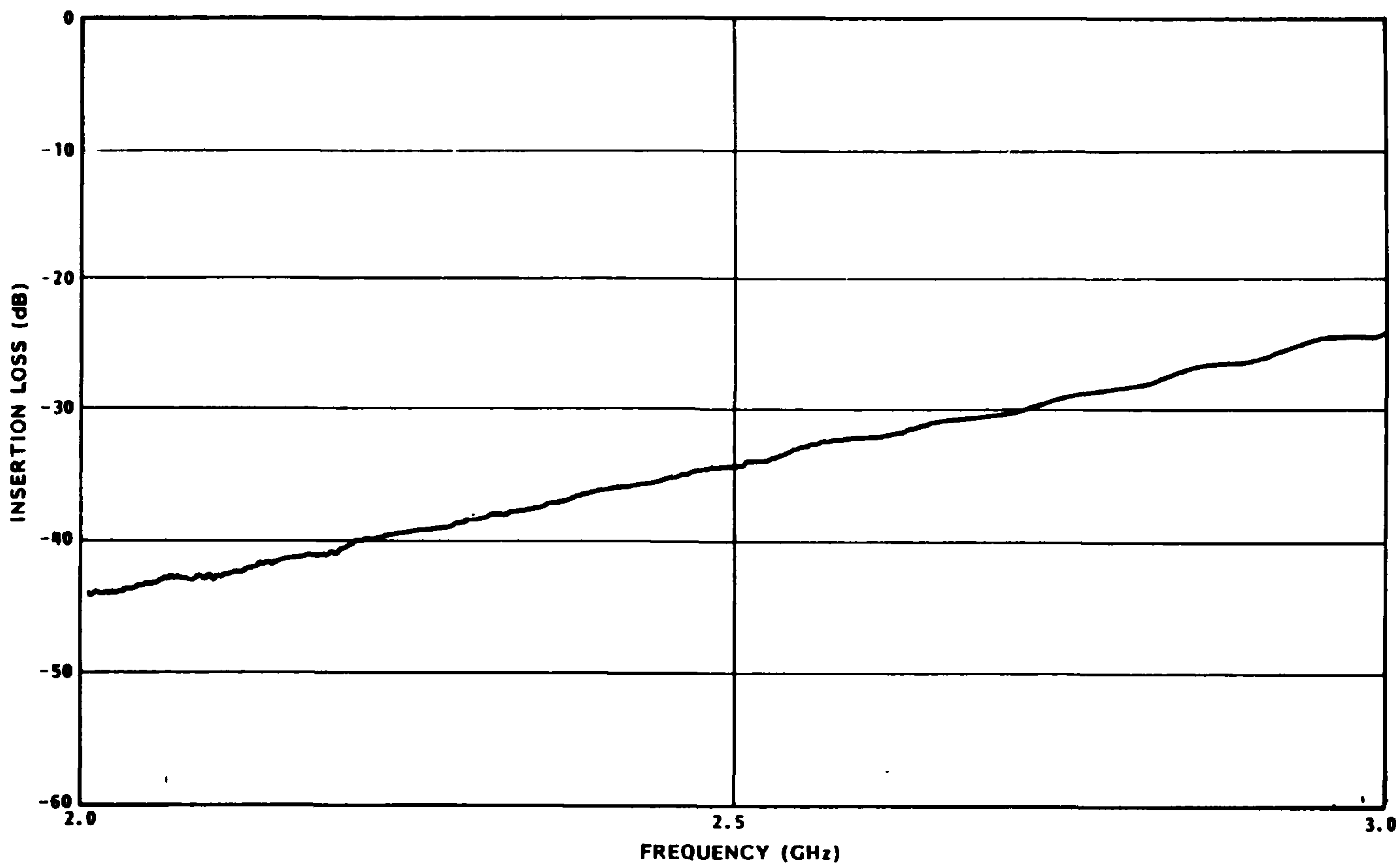

Figure 4-20. Electromagnetic Feedthrough in HC-37 Can (2 to 3 GHz)

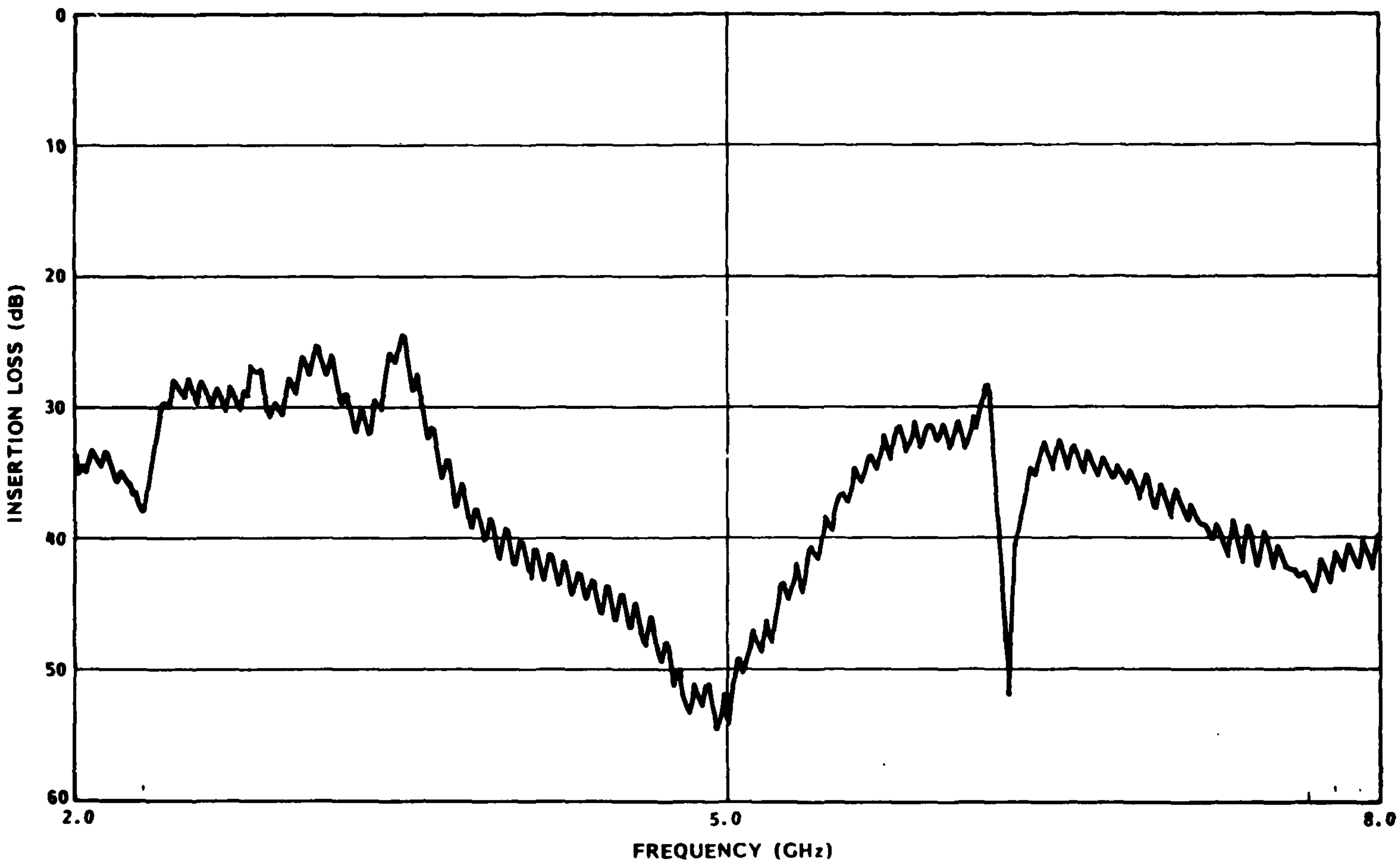

Figure 4-21. Electromagnetic Feedthrough in Ceramic Flatpack

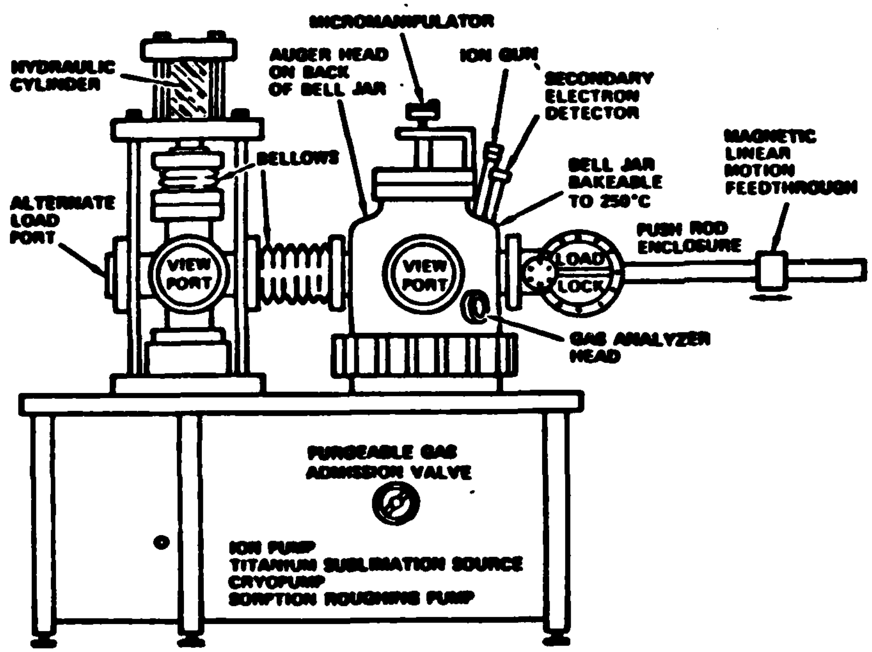

- o ULTRAHIGH VACUUM (10^{-9} TORR)
- o BAKEABLE TO 250°C
- o AUGER PROBE
- o GAS ANALYZER
- o ION GUN FOR SURFACE CLEANING
- o GAS LEAK VALVE
- o HIGH VACUUM TRANSPORT FROM SURFACE ANALYSIS TO COLD WELD PRESS

Figure 4-22. **Surface Analysis and Cold Welding System**

This system involves connecting the Varian Model 981-2001 ultra-high vacuum surface analysis chamber to the vacuum chamber of the Associated General Laboratories Unit. The SBAW device can be analyzed in the Varian chamber and, if unsatisfactory, be discarded or given additional UV cleaning. The cleaned devices will then be transferred to the cold weld side through a manipulator and sealed. In this manner, control on the cleanliness of the device will be established.

5.0 SBAW OSCILLATOR CIRCUIT DESIGN

The general form of a SBAW delay line oscillator is as shown in Figure 5-1. The conditions for oscillation are (1) gain around the loop must exceed all losses, and (2) phase around the loop must equal a multiple of 2π radians. These conditions can be expressed as

$$L_S(f) + L_I(f) \leq G(f,A) \qquad (5.1)$$

and

$$\frac{2\pi f_N \ell}{V} + \phi = 2N\pi \qquad (5.2)$$

where

f_N = oscillation frequencies
ℓ = center-to-center transducer separation
V = SBAW velocity
ϕ = phase shift through all elements except SBAW delay line
N = an integer
$L_S(f)$ = insertion loss of SBAW delay line
$L_I(f)$ = insertion loss of feedback loop components
$G(f,A)$ = amplifier gain as a function of f and output level, A
A = output power level

The frequency of oscillation can be determined from Equation (5.2)

$$f_N = \frac{V}{\ell}\left(N - \frac{\phi}{2\pi}\right) \qquad (5.3)$$

It is possible for multiple solutions to Equations (5.1) and (5.2) to exist where many solutions to the phase condition exist within the SBAW passband. For single-mode operation, the SBAW delay line is designed such that there is only one solution for Equation (5.2) which is in the passband of the delay line. Such a design is shown in Figure 5-2. As a general rule, the loss associated with the feedback loop components, $L_I(f)$, and the amplifier gain, $G(f,A)$, are slowly varying functions of frequency over a broad range around the frequency for which the oscillator is being designed, and the SBAW response, $L_S(f)$, is a very strong function of frequency. The SBAW oscillator is designed so that the combination

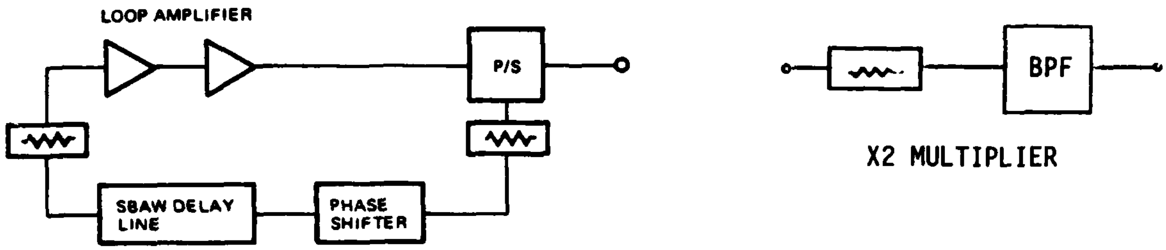

Figure 5-1. SBAW Delay Line Oscillator

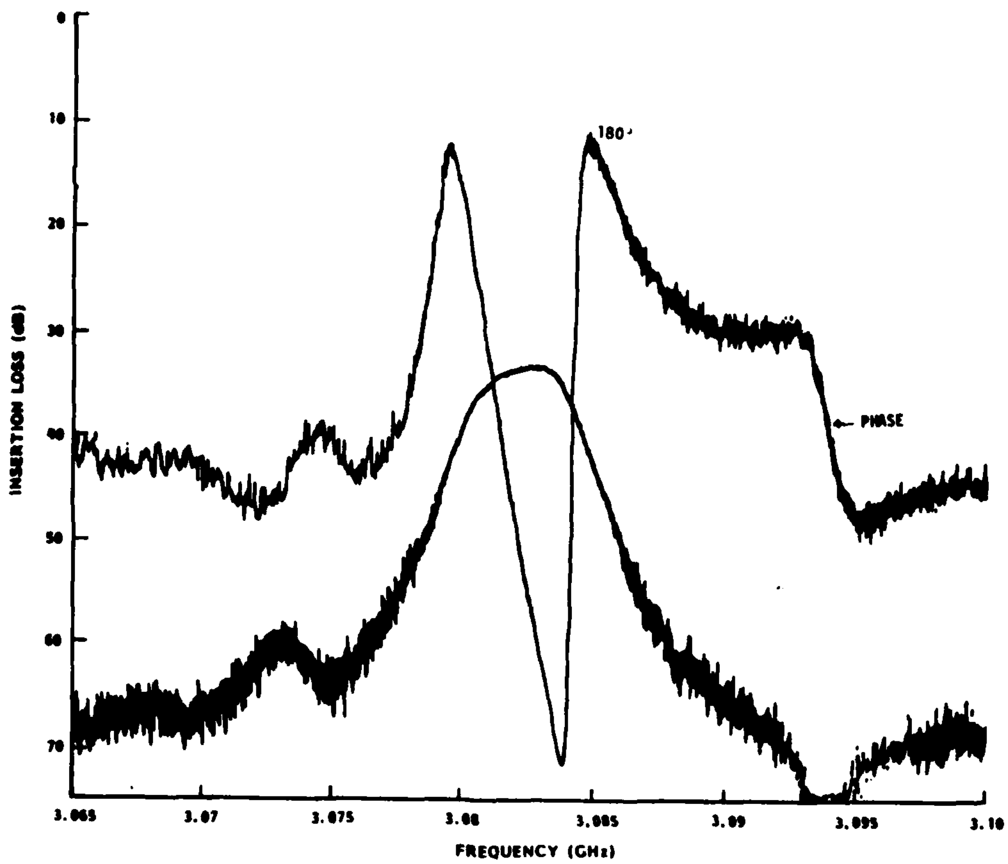

Figure 5-2. Single Mode SBAW Delay Line

of SBAW delay line loss plus amplifier gain exceeds unity over a desired frequency band around the desired operating frequency. As long as only one solution to (5.2) falls within the passband response of the SBAW delay line, single mode operation of the SBAW oscillator is guaranteed.

The loop amplifier shown in Figure 5-1 provides gain to overcome losses around the loop - thereby meeting the first condition for oscillation (Equation (5.1)). The amplifier is designed to have linear gain well in excess of the loop losses. The required gain margin is a function of the saturation characteristics of the amplifier chain, but typically must be greater than 4 dB. Measurements made at TRW have shown that a minimum of 4 dB gain margin will provide maximum output power and minimum phase noise. For a circuit with adequate gain margin, the oscillator output power will equal the saturated output power of the amplifier minus the power coupled back into the loop. The second condition for oscillation, Equation (5.2), is met through use of the phase shifter shown in Figure 5-1. The frequency of oscillation is set by varying ϕ in Equation (5.3).

Since the goal of this program is not only to design S-band and X-band SBAW oscillators but to ultimately utilize them in advanced systems where excellent frequency stability is a necessity, the oscillator electronic circuitry and layout will be designed with emphasis on achieving this stability. It should be noted that relative to bulk crystal oscillators, which typically have Qs of 10^6, the Qs of SBAW delay lines are much lower, typically in the thousands. Therefore, the effects of electronics drift are several orders of magnitude more sensitive for a SBAW (or SAW) oscillator than for a bulk crystal oscillator. As an example, the delay in a SBAW oscillator delay line is about 1 μsec, which does not truly negate the effects of delay variation in other loop components. It is not unusual for delay in the loop electronic components to be 20 nsec, creating a situation where a 1% change in electronic component delay would produce approximately 200 ppm oscillator frequency variation. Similar electronic variations in a bulk oscillator would produce only a fraction of a ppm frequency variation. It is therefore very important in the design of SBAW oscillators on this program to minimize variations in electronic components and circuits. Hence, the

design of the amplifier will be distributed (MIC on alumina) where feasible to minimize lumped elements. No series lumped matching will be used since gain and transmission phase tend to be more sensitive to variation in series components. The lumped components which are used will be components with low aging rates. Glass or NPO ceramic capacitors, and thick film resistors will be used. Air coil inductors will not be used in matching networks. The amplifier design will be broadband and precautions will be taken to assure out-of-band stability. Often out-of-band stability is a problem in SBAW oscillators since the SBAW delay lines present poor out-of-band reflection coefficients. The use of attenuators in the loop will assure stability. By careful consideration of these principles, and screening the circuit design, certain commercially available hybrid amplifiers can be used to minimize development costs.

The performance specifications for the amplifiers selected are listed in Table 5-1.

The power splitter will be a resistive divider since circuits of this type are broadband in both amplitude and phase characteristics. The phase adjustment network will be a length of transmission line which is adjustable through wire bonding or ribbon bonding. The attenuators will be "π" or "T" pads using thick film chip resistors. The attenuators, in addition to assuring stability, set the power level into the SBAW, and set loop gain margin. The gain budgets for the three SBAW oscillators are listed in Table 5-2.

Table 5-1. Amplifier Performance Specifications

Description	Manufacturer/Model No.	Noise Figure (dB)	Small Signal Gain (dB)	Output Power (dBm)	Frequency Range (GHz)
1680 MHz Oscillator	W-J R14-951	4.0	18	+10	1.0 - 2.0
S-Band Oscillator	Aertech A55F-402	4.0	20	+10	2.0 - 4.0
	Aertech A55F-403	4.0	32	+10	2.0 - 4.0
X-Band Oscillator	Aertech A55H-5C6	5.0 max.	50 min.	+10 min.	4.0 - 8.0

Table 5-2. Oscillator Gain Budgets

	1680 MHz	S-Band	X-Band
Amplifier Gain (dB)	36.0	52.0	50.0
SBAW Loss	-25.0	-32.0	-40.0
Power Splitter Loss	- 6.0	- 6.0	- 3.0
Phase Shifter Loss	- 0.2	- 0.2	- 0.3
Attenuator Loss	- 0.8	- 9.8	- 2.7
Gain Margin (dB)	+ 4.0	+ 4.0	+ 4.0

6.0 CONCLUSIONS AND PROJECTED PLANS

This first annual report describes the technical progress of the program for the period of September 1981 through August 1982. The major activities for this period were the examination of system applications, SBAW device investigation, SBAW device fabrication, and oscillator circuit design considerations.

Several systems have been identified in which the use of high frequency SBAW oscillators will greatly improve system performance. From the system study, it is clear that as more and more weapon systems move to millimeter wave frequencies, there will be an increasing requirement for stable, low noise frequency sources and precision test equipment. SBAW technology will provide the devices which will be needed to meet this challenge.

In the SBAW device investigation, the parameters studied were material aspects, metallization effect, transducer configuration, equivalent circuit and harmonic operation. This task is essentially complete. The fabrication methods described have been used to fabricate devices on both AT and BT quartz. The 3 GHz fundamental mode delay uses a simple one-up, one-down finger configuration, and is fabricated on AT quartz. Both the 3.5 GHz 5th harmonic devices on BT quartz and the 5 GHz 5th harmonic devices on AT quartz use a 6-finger/period pattern. All three delay lines have transducer linewidths and spaces of 0.4 μm and to date have used e-beam direct writing. Masks are being written and a process developed to use shallow uv light contact photolithography to fabricate these devices. The 9.9 GHz delay line will use 3 finger/period patterns on AT quartz and operate at the secondary response. Its linewidth will be 0.6 μm, and it will be fabricated using the e-beam direct-writing process. The AT quartz harmonic delay lines will use an embedded transducer structure with aluminum metallization 300-450 Å. The delay lines are also predicted to have turnover temperatures near room temperature, and will have second order temperature stability around 50×10^{-9} °C^2 (AT).

Mounting and packaging studies have been completed, and the HC-37 package selected for use. Delay lines meeting the program objectives will be sealed with TRW's cold welder system, which combines surface analysis and device packaging in one system. Then stable oscillators will be constructed and aging studies commenced.

The oscillator circuit design process and considerations have been outlined, and the fabrication process started. The circuits will be ready in the near future, as the optimized delay lines are produced.

During the next reporting period, SBAW delay line fabrication will be completed, and oscillator investigation will be addressed. Major tasks which will be accomplished include:

- Completion of 3 GHz, 3.5 GHz, 5 GHz and 10 GHz delay line fabrication
- 1680 MHz SBAW delay line fabrication
- Completion of 3 GHz, 3.5 GHz, 5 GHz and 10 GHz oscillator circuit
- Completion of 1680 MHz oscillator circuit.
- Construction of 3 GHz, 5 GHz, 10 GHz and 1680 MHz SBAW oscillators.
- Commencement of oscillator characterization and aging studies.

REFERENCES

1. T. E. Parker, "1/f Phase Noise in Quartz Delay Lines and Resonators," 1979 Ultrasonics, pp. 878-881, Hewlett-Packard 10811 Crystal Oscillator.

2. K. F. Lau, K. H. Yen, R. S. Kagiwada, and A. M. Kong, "High Frequency Temperature Stable SBAW Oscillators," Proceedings, IEEE 1980 Ultrasonics Symposium, pp. 240-244.

3. K. H. Yen, K. F. Lau and R. S. Kagiwada, "Recent Advances in Shallow Bulk Acoustic Wave Devices," Proceedings, IEEE 1979 Ultrasonics Symposium, pp. 776-785.

4. T. J. Lukaszek, A. Ballato, K. H. Yen and R. S. Kagiwada, "SAW and SBAW on Doubly Rotated Cut Quartz," Proceedings, IEEE 1979 Ultrasonics Symposium, pp. 797-801.

5. A. Ballato and T. J. Lukaszek, "Shallow Bulk Acoustic Wave Progress and Prospects," IEEE Trans. Microwave Theory and Techniques, MTT-27, 1979, pp. 1004-1012.

6. A. Ballato and T. J. Lukaszek, "Shallow Bulk Acoustic Wave Devices," IEEE 1979 MTT Digest, pp. 162-164.

7. A. J. Slobodnik, Jr., and J. V. O'Brien, "Complete Theory of Acoustic Bulk Wave Propagation in Anisotropic Piezoelectric Media," Air Force Cambridge Research Laboratories, AFCRL-71-0601, 24 November, 1971, Physical Sciences Research Paper, No. 468.

8. T. Nishikawa, A. Tani, K. Shirai and C. Takeuchi, "SH-Type Surface Acoustic Waves on Rotated Y-Cut Quartz," Proceedings, 1980 Frequency Control Symposium, pp. 286-291.

9. J. Z. Wilcox and K. H. Yen, "Shear Horizontal Surface Wave on Rotated Y-Cut Quartz," IEEE Trans. Sonics and Ultrasonics, November, 1981.

10. R. D. Weglein and O. W. Otto, "Microwave SAW Oscillators," Proceedings, IEEE 1977 Ultrasonics Symposium, pp. 913-922.

11. H. Engan, "SAW Multielectrode Transducers," IEEE Trans. Sonics and Ultrasonics, 1975, Vol. SU-22, pp. 395-401.

12. J. R. Vig, "UV/Ozone Cleaning of Surfaces: A Review," <u>Surface Contamination, Genesis, Detection and Control</u>, Vol. 2, Ed. by K. L. Miltal, Plenum Press, 1979, p. 235.

13. K. V. Rousseau, K. H. Yen, K. F. Lau, and A. M. Kong, to be published.

14. R. L. Filler, J. R. Vig, L. J. Keres, and T. M. Snowden, "Ceramic Flatpack Enclosed AT-and SC-Cut Resonators," Roceedings, IEEE 1980 Ultrasonics Symposium, pp. 819-824.

DISTRIBUTION LIST

ELECTRONICS TECHNOLOGY AND DEVICES LABORATORY
MANDATORY CONTRACT DISTRIBUTION LIST

101 Defense Technical Information Center
ATTN: DTIC-TCA
Cameron Station (Bldg 5)
012 Alexandria, VA 22314

203 GIDEP Engineering & Support Dept
TE Section
PO Box 398
001 NORCO, CA 91760

205 Director
Naval Research Laboratory
ATTN: CODE 2627
001 Washington, DC 20375

301 Rome Air Development Center
ATTN: Documents Library (TILD)
001 Griffiss AFB, NY 13441

437 Deputy for Science & Technology
Office, Asst Sec Army (R&D)
001 Washington, DC 20310

438 HQDA (DAMA-ARZ-D/Dr. F.D. Verderame)
001 Washington, DC 20310

482 Director
US Army Materiel Systems Analysis Actv
ATTN: DRXSY-MP
001 Aberdeen Proving Ground, MD 21005

563 Commander, DARCOM
ATTN: DRCDE
5001 Eisenhower Avenue
001 Alexandria, VA 22333

564 Cdr, US Army Signals Warfare Lab
ATTN: DELSW-OS
Vint Hill Farms Station
001 Warrenton, VA 22186

705 Advisory Group on Electron Devices
201 Varick Street, 9th Floor
002 New York, NY 10014

579 Cdr, PM Concept Analysis Centers
ATTN: DRCPM-CAC
Arlington Hall Station
001 Arlington, VA 22212

602 Cdr, Night Vision & Electro-Optics
ERADCOM
ATTN: DELNV-D
001 Fort Belvoir, VA 22060

603 Cdr, Atmospheric Sciences Lab
ERADCOM
ATTN: DELAS-SY-S
001 White Sands Missile Range, NM 88002

607 Cdr, Harry Diamond Laboratories
ATTN: DELHD-CO, TD (In Turn)
2800 Powder Mill Road
001 Adelphi, MD 20783

609 Cdr, ERADCOM
ATTN: DRDEL-CG, CD, CS (In Turn)
2800 Powder Mill Road
001 Adelphi, MD 20783

612 Cdr, ERADCOM
ATTN: DRDEL-CT
2800 Powder Mill Road
001 Adelphi, MD 20783

680 Commander
US Army Electronics R&D Command
000 Fort Monmouth, NJ 07703
1 DELET-MQ
1 DELEW-D
1 DELET-DD
1 DELSD-L (Tech Library)
2 DELSD-L-S (STINFO)
10 DELET-MA-A
1 DELET-MF

681 Commander, CECOM
Fort Monmouth, NJ 07703

001 Fort Monmouth, NJ 07703

ELECTRONICS TECHNOLOGY AND DEVICES LABORATORY
SUPPLEMENTAL CONTRACT DISTRIBUTION LIST

103 Code R123, Tech Library
DCA Defense Comm Engrg Ctr
1800 Wiehle Ave
001 Reston, VA 22090

104 Defense Communications Agency
Technical Library Center
Code 205 (P. A. Tolovi)
001 Washington, DC 20305

206 Commander
Naval Electronics Laboratory Center
ATTN: Library
001 San Diego, CA 92152

207 Cdr, Naval Surface Weapons Center
White Oak Laboratory
ATTN: Library Code WX-21
001 Silver Spring, MD 20910

314 Hq, Air Force Systems Command
ATTN: DLCA
Andrews Air Force Base
001 Washington, DC 20331

403 Cdr, MICOM
Redstone Scientific Info Center
ATTN: Chief, Document Section
001 Redstone Arsenal, AL 35809

406 Commandant
US Army Aviation Center
ATTN: ATZQ-D-MA
001 Fort Rucker, AL 36362

407 Director, Ballistic Missile Defense
Advanced Technology Center
ATTN: ATC-R, PO Box 1500
001 Huntsville, AL 35807

418 Commander
HQ, Fort Huachuca
ATTN: Technical Reference Div
001 Fort Huachuca, AZ 85613

475 Cdr, Harry Diamond Laboratories
ATTN: Library
2800 Powder Mill Road
001 Adelphi, MD 20783

477 Director
US Army Ballistic Research Labs
ATTN: DRXBR-LB
001 Aberdeen Proving Ground, MD 21005

455 Commandant
US Army Signal School
ATTN: ATZH-CD
001 Fort Gordon, GA 30905

422 Commander
US Army Yuma Proving Ground
ATTN: STEYP-MTD (Tech Library)
001 Yuma, AZ 85364

507 Cdr, AVRADCOM
ATTN: DRSAV-E
PO Box 209
001 St. Louis, MO 63166

511 Commander, Picatinny Arsenal
ATTN: SARPA-FR-5, -ND-A-4,
-TS-S (In Turn)
001 Dover, NJ 07801

515 Project Manager, REMBASS
ATTN: DRCPM-RBS
001 Fort Monmouth, NJ 07703

517 Commander
US Army Satellite Communications Agcy
ATTN: DRCPM-SC-3
001 Fort Monmouth, NJ 07703

518 TRI-TAC Office
ATTN: TT-SE
001 Fort Monmouth, NJ 07703

ELECTRONICS TECHNOLOGY AND DEVICES LABORATORY
SUPPLEMENTAL CONTRACT DISTRIBUTION LIST (CONT)

519 Cdr, US Army Avionics Lab
AVRADCOM
ATTN: DAVAA-D
001 Fort Monmouth, NJ 07703

520 Project Manager, FIREFINDER
ATTN: DRCPM-FF
001 Fort Monmouth, NJ 07703

521 Commander
Project Manager, SOTAS
ATTN: DRCPM-STA
001 Fort Monmouth, NJ 07703

531 Cdr, US Army Research Office
ATTN: DRXRO-PH (Dr. Lontz)
DRXRO-IP (In Turn)
PO Box 12211
001 Research Triangle Park, NC 27709

556 HQ, TCATA
Technical Information Center
ATTN: Mrs. Ruth Reynolds
001 Fort Hood, TX 76544

568 Commander
US Army Mobility Eqp Res & Dev Cmd
ATTN: DRDME-R
001 Fort Belvoir, VA 22060

604 Chief
Ofc of Missile Electronic Warfare
Electronic Warfare Lab, ERADCOM
001 White Sands Missile Range, NM 88002

606 Chief
Intel Materiel Dev & Support Ofc
Electronic Warfare Lab, ERADCOM
001 Fort Meade, MD 20755

608 Commander
ARRADCOM
DRDAR-TSB-S
001 Aberdeen Proving Ground, MD 21005

614 Cdr, ERADCOM
ATTN: DRDEL-LL, -SB, -AP (In Turn)
2800 Powder Mill Road
001 Adelphi, MD 27083

617 Cdr, ERADCOM
ATTN: DRDEL-AQ
2800 Powder Mill Road
001 Adelphi, MD 20783

619 Cdr, ERADCOM
ATTN: DRDEL-PA, -ILS, -ED (In Turn)
2800 Powder Mill Road
001 Adelphi, MD 20783

703 NASA Scientific & Tech Info Facility
Baltimore/Washington Intl Airport
001 PO Box 8757, MD 21240

704 National Bureau of Standards
Bldg 225, RM A-331
ATTN: Mr. Leedy
001 Washington, DC 20231

ELECTRONICS TECHNOLOGY AND DEVICES LABORATORY

SUPPLEMENTAL CONTRACT DISTRIBUTION LIST (CONT)

Commander, AFAL
ATTN: Mr. W. J. Edwards, TEA
Wright-Patterson AFB, Ohio 45433 (1)

D. Chrissotimos, Code 727
National Aeronautics & Space Administration
Goddard Space Flight Center
Greenbelt, MD (1)

Naval Research Laboratories
Code 5237
Washington, DC 20375
ATTN: Dr. D. Webb (1)

HQ ESD (DRI)
L. G. Hanscom AFB
Bedford, MA 01731 (1)

US Army Missile Command
DRSMI-REL
Redstone Arsenal, AL 35809
ATTN: G. J. Rast, Jr. (1)

Commander, MICOM
ATTN: DRSMI-RE (Mr. Pittman)
Redstone Arsenal, AL 35809 (1)

Commander, ERADCOM
ATTN: DRDEL-IL-S
2800 Powder Mill Road
Adelphi, MD 20783 (1)

Coordinated Science Laboratory
University of Illinois
Urbana, Illinois 61801
ATTN: Dr. Bill J. Hunsinger (1)

General Electric Co.
Electronics Lab
Electronics Park
Syracuse, NY 13201
ATTN: Mr. S. Wanuga (1)

Anderson Laboratories, Inc.
1280 Blue Hills Avenue
ATTN: Dr. A. A. Comparini
Bloomfield, Conn. 06002 (1)

Texas Instruments, Inc.
P. O. Box 5936
13500 N. Central Expressway
Dallas, Texas 75222
ATTN: Dr. L. T. Clairborne (1)

Sperry Rand Research Center
100 North Road
Sudbury, Massachusetts 01776
ATTN: Dr. H. Van De Vaart (1)

Raytheon Company
41 Spring Street
Lexington MA 02173
ATTN: Dr. T. Parker (1)

Westinghouse Electric Corp.
Research & Development Center
Beulah Road
Pittsburgh, PA 15235
ATTN: Dr. B. McAvoy (1)

TRW
Defense and Space Sys Group
One Space Park
Redondo Beach, CA 90278
ATTN: Dr. R. S. Kagiwada (1)

Dr. F. Cho
Integrated Circuit Facility
Motorola Government Electronics Div.
8201 East McDowell Road
Scottsdale, AZ 85257 (1)

McGill University
ATTN: G. W. FArnell
Montreal 110, Canada (1)

United Aircraft Research Labs
ATTN: Dr. Thomas W. Grudkowski
East Hartford, Conn. 06108 (1)

Science Center
Rockwell International
Thousand Oaks, CA 91360
ATTN: Dr. E. Staples (1)

AMES Laboratory
215 Reactor Bldg
Iowa State University
Ames, Iowa 50011
ATTN: Dr. K. Lakin (1)

SAWTEK, Inc.
P. O. Box 7756
2451 Shader Road
Orlando, Florida 32854
ATTN: Mr. S. Miller (1)

Dr. William R. Shreve
HP Laboratories
1501 Page Mill Road
Palo Alto, CA 94304 (1)

DATE
FILMED

-8